The Abdus Salam
International Centre for Theoretical Physics

United Nations
Educational, Scientific
and Cultural Organization

International Atomic
Energy Agency

SMR/1758-13

"Workshop on Ion Beam Studies of Nanomaterials:
Synthesis, Modification and Characterization"

26 June - 1 July 2006

# Energy transfer from metal nanostructures to rare earth: applications in photonics

*Enrico Trave*
*Department of Physics "G. Galilei"*
*University of Padova*
*Padova, Italy*

Strada Costiera 11, 34014 Trieste, Italy - Tel. +39 040 2240 111; Fax +39 040 224 163 - sci_info@ictp.it, www.ictp.it

# *Energy transfer from metal nanostructures to rare earth: applications in photonics*

**Enrico Trave**

**Department of Physics "G. Galilei"**

**University of Padova**

# Er doped materials: the optical network

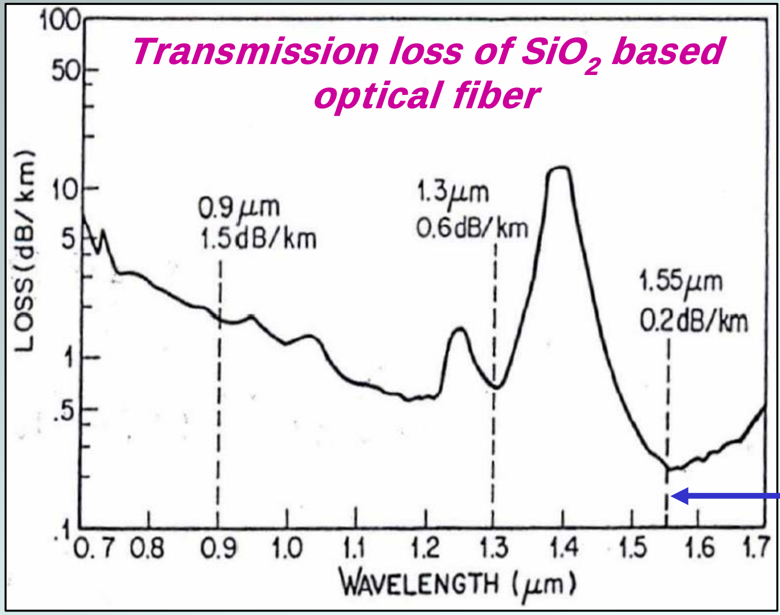


$Er^{3+}$ emission at 1.54 µm

The optical communication technology is largely interested in Er doped materials

1987: demonstration of the feasibility of Er doped fiber amplifier (EDFA)

- great development of optical communication technology
- setting of $Er^{3+}$ transition at 1.54 µm as one of the standard communication wavelength

Next step: realization of a planar amplifier, in which Er doped waveguides can be integrated with other optical components such as lasers, splitters, modulators or multiplexers on a single optical circuit

# Sensitizers for Er

In the small length of planar integrated devices (few cm), high Er density and high pumping efficiency is required to get reasonable gain values

Limit of Er doped materials for light amplification: small cross section for optical excitation → Increase the Er ion pumping efficiency through energy coupling with optically excited sensitizers

Different concepts of Er sensitizers:

- ✓ Rare earths (Yb,...)
- ✓ Silicon nanostructures
- ✓ Organic complexes
- ✓ **Metals (Ag,Au)**

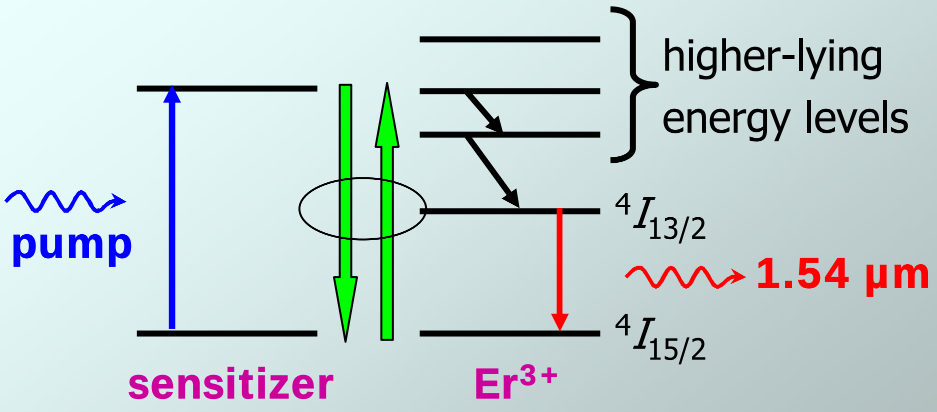

# Metal as sensitizers for rare earth ions

✓ Eu and Ag codoped $SiO_2$ sol-gel films — ***T. Hayakawa et al., Appl. Phys. Lett. 74, 1513 (1999)***

Rare earth fluorescence increases by a local field enhancement due to SPR of Ag nanoparticles (<D>=4.3 nm)

✓ Er implanted Ag-exchanged borosilicate glasses — ***C. Strohhöfer et al., Appl. Phys. Lett. 81, 1414 (2002)***

Ag-related sensitizers (multimers, pairs of Ag ions/atoms) induce the enhancement of $Er^{3+}$ emission through light absorption and subsequent energy transfer process

✓ Er and Au codoped $SiO_2$ sol-gel films — ***M. Fukushima et al., J. Appl. Phys. 98, 024316 (2005)***

Au nanoparticles (<D>=20 nm) can activate the enhancement of $Er^{3+}$ emission by the interaction with the strong field induced by SPR

# Investigation on Er and metal codoped systems

✓ **Er and Ag coimplantation in silica**

✓ **Er and Au coimplantation in silica**

✓ **Ag-exchanged Er doped sol-gel films**

★ Er doped glasses: rare earth optical behaviour

★ Metal codoping: impact on Er luminescence activity

★ Er sensitization mechanism

★ Evaluation of the effective $Er^{3+}$ excitation cross section

## Er implantation in silica

# Er implantation in silica

**Er**

| Fluence | Energy | Annealing (in $N_2$) |
|---|---|---|
| $6.8\times10^{14}$ at/cm$^2$ | 50+100+190 keV | 600→1000°C, 1h |

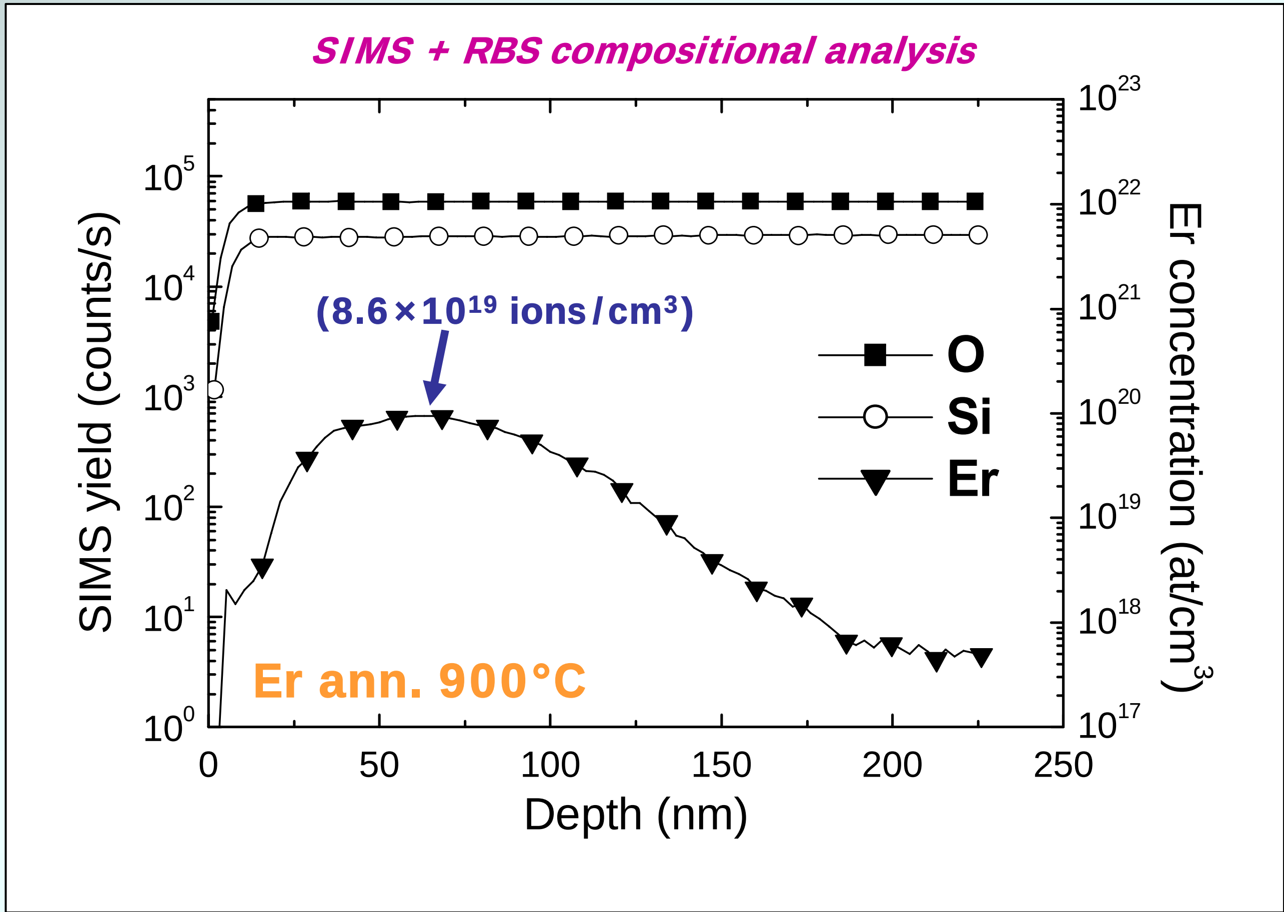

# Er PL emission at 1.54 μm

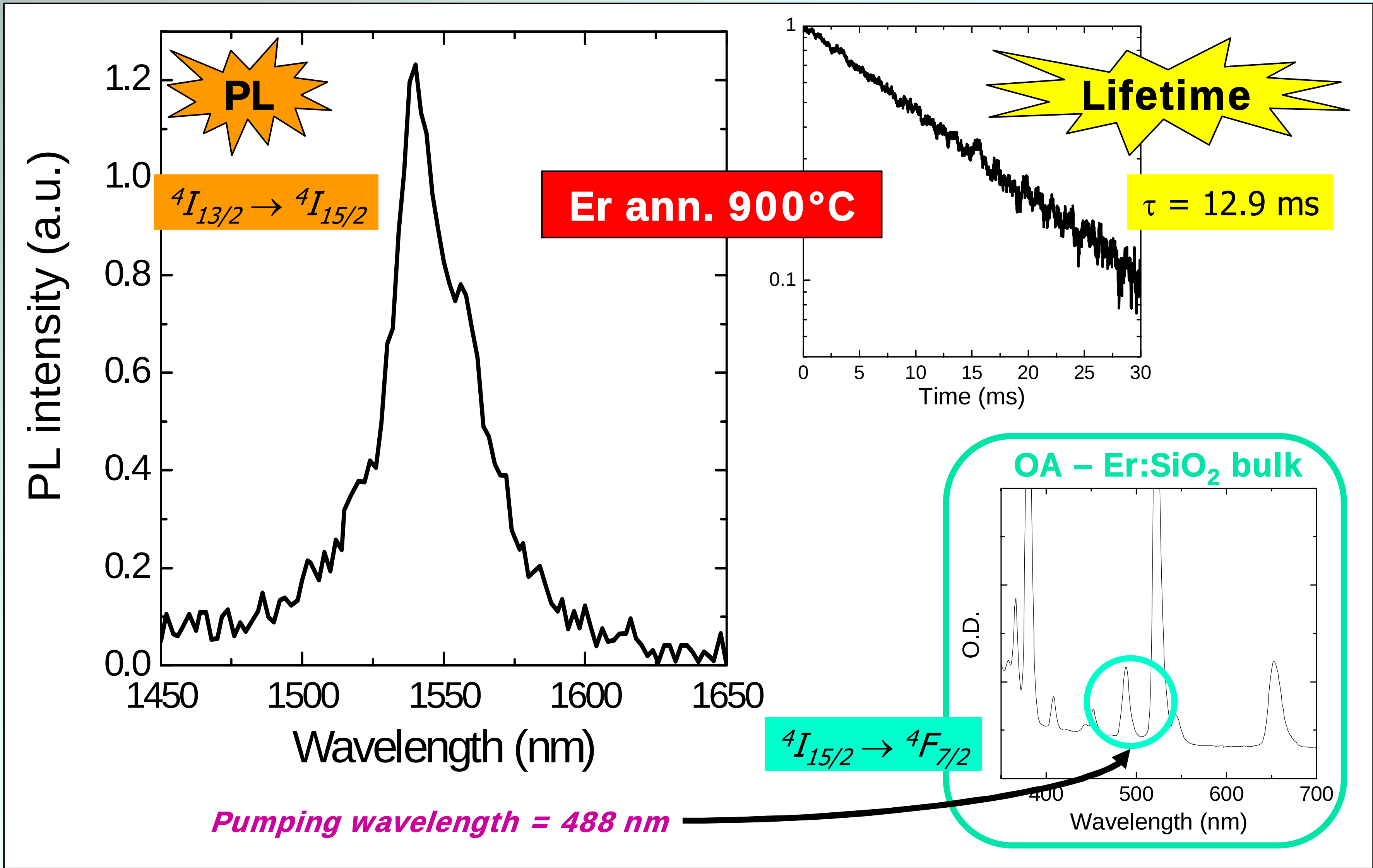

# PL vs annealing temperature

$$I_{PL} \propto N_{act}\eta$$

- $N_{act}$: Concentration of optically active $Er^{3+}$
- $\eta$: PL quantum efficiency $\eta = \frac{\tau}{\tau_{rad}}$
  - $\tau$ ← *lifetime*
  - $\tau_{rad}$ ← *~25 ms in silica*

$$I_{PL} \propto \tau$$

Recovery of the matrix damaged by implantation

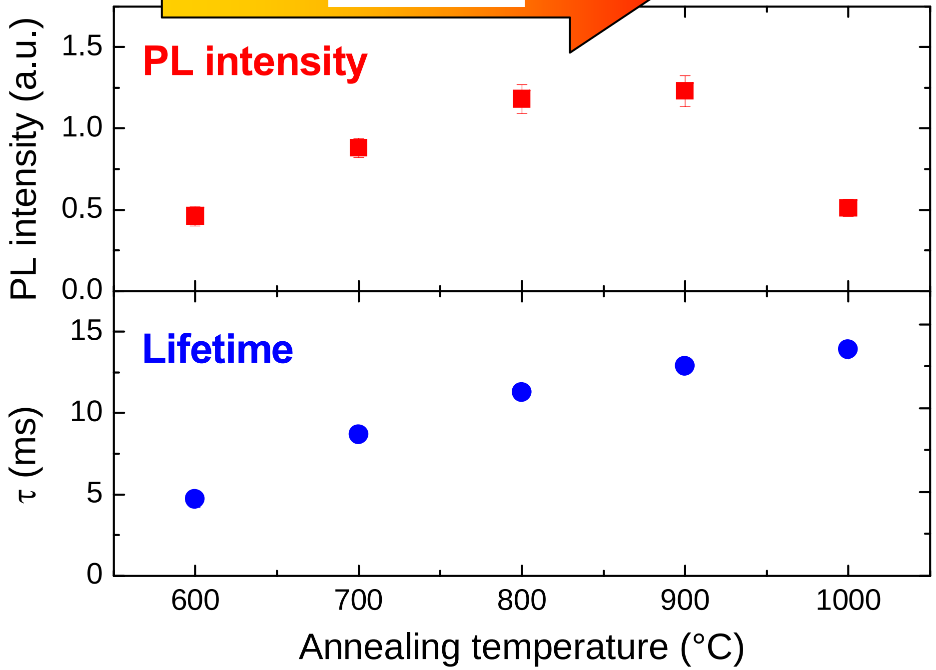

# PL vs annealing temperature

$$I_{PL} \propto N_{act}\eta$$

- Concentration of optically active $Er^{3+}$
- PL quantum efficiency $\eta = \frac{\tau}{\tau_{rad}}$ — $\tau$: *lifetime*; $\tau_{rad}$: *~25 ms in silica*

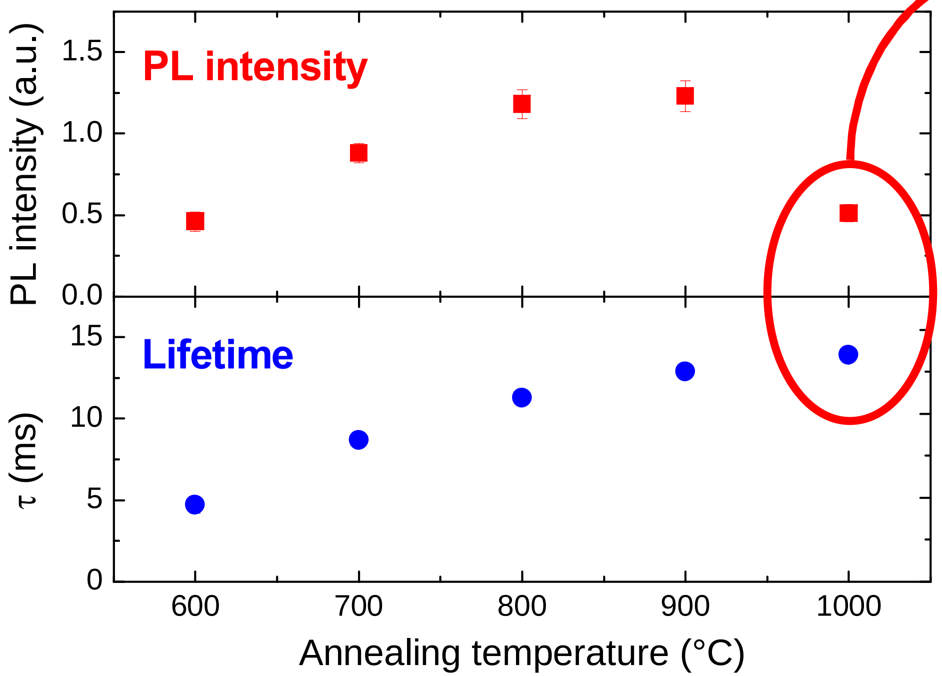


$N_{act}$ decreases?

Er-O clustering at 1000°C?

*EXAFS at Er $L_{III}$-edge*

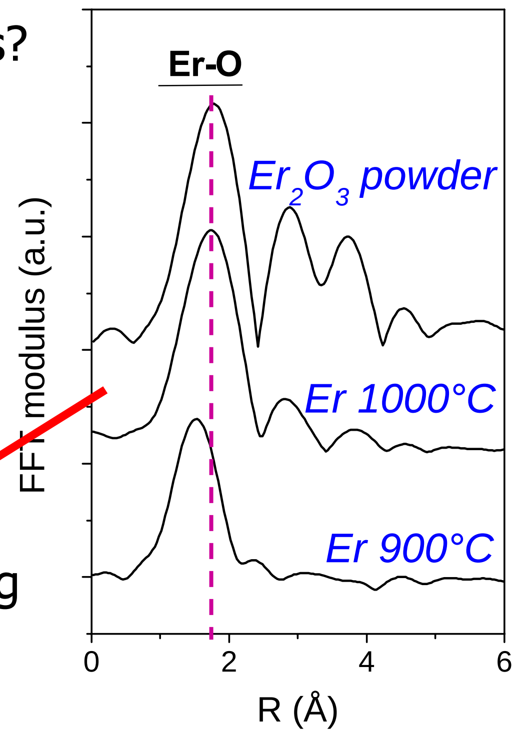

# Er and Ag coimplantation in silica

# Er and Ag coimplantation in silica

**Er**

| Fluence | Energy | Annealing (in $N_2$) |
|---|---|---|
| $6.8\times10^{14}$ at/cm$^2$ | 50+100+190 keV | 900°C, 1h |

+

**Ag**

| Fluence | Energy | Annealing (in $N_2$) |
|---|---|---|
| $6.1\times10^{15}$ at/cm$^2$ | 45+90+190 keV | 400→900°C, 1h |

**Thermal treatment:**

- ✓ Matrix recovery
- ✓ Activation of metal migration and aggregation processes

★ *Structural and optical measurements*

Evolution of Ag aggregation

★ *PL investigation*

Er luminescence behaviour

# Compositional characterization

**Er**

| Fluence | Energy | Annealing (in $N_2$) |
|---|---|---|
| $6.8\times10^{14}$ at/cm$^2$ | 50+100+190 keV | 900°C, 1h |

**+**

**Ag**

| Fluence | Energy | Annealing (in $N_2$) |
|---|---|---|
| $6.1\times10^{15}$ at/cm$^2$ | 45+90+190 keV | 400→900°C, 1h |

***SIMS + RBS compositional analysis***

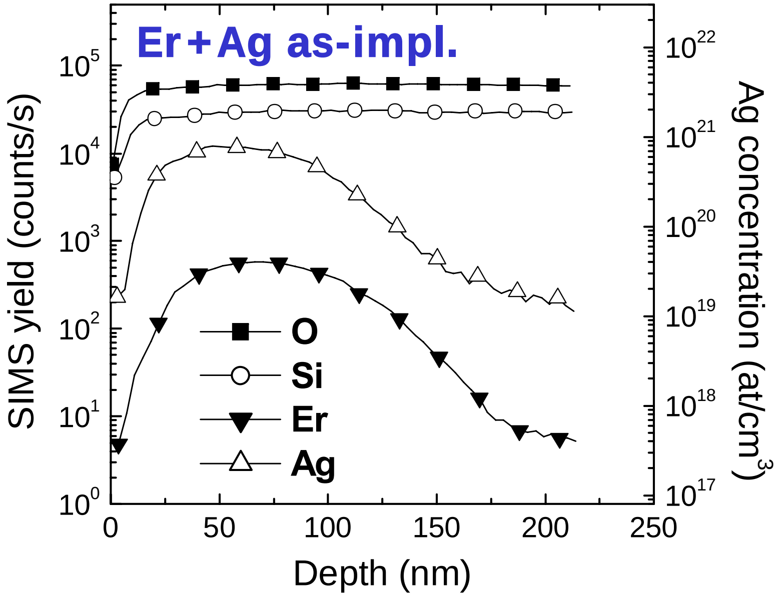


- ✓ Ag and Er profiles overlapped after implant
- ✓ After annealing, Ag profile moving towards the surface
- ✓ Ag conc. and dose decrease with annealing T

| | *conc. ($Ag^+/cm^3$)* | *dose ($Ag^+/cm^2$)* |
|---|---|---|
| **as-impl.** | $8.2\times10^{20}$ | $6.1\times10^{15}$ |
| **ann. 900°C** | $4.3\times10^{20}$ | $2.7\times10^{15}$ |

# TEM analysis

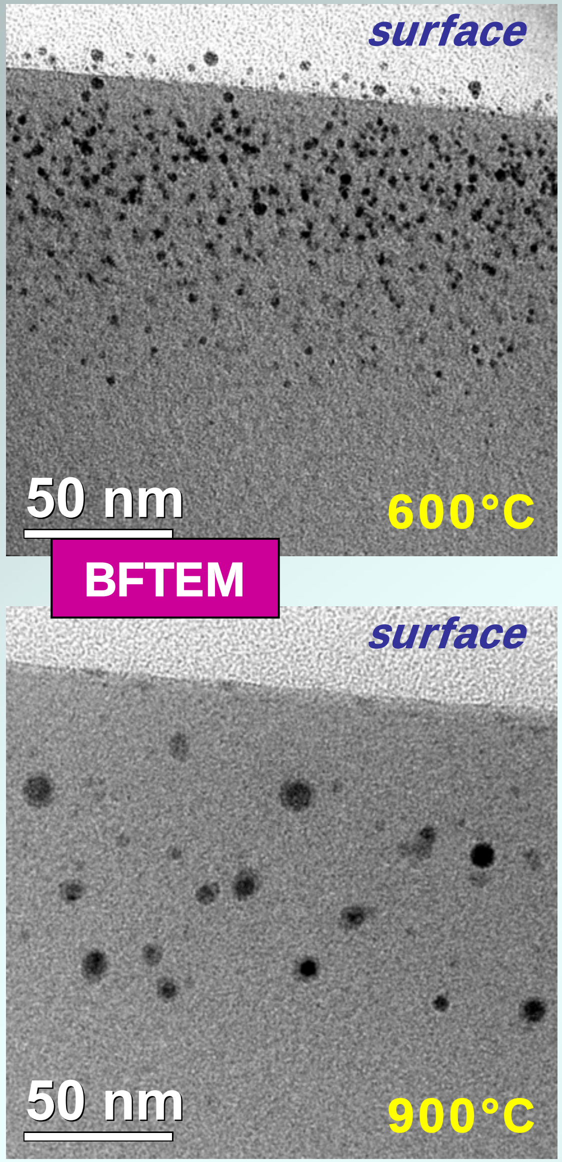


- ✓ Precipitation of Ag clusters
- ✓ Metal concentration centroid moves towards the surface
- ✓ Formation of clusters on the surface
- ✓ Cluster size increases with the annealing T

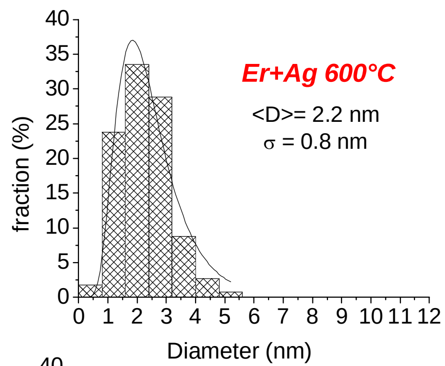


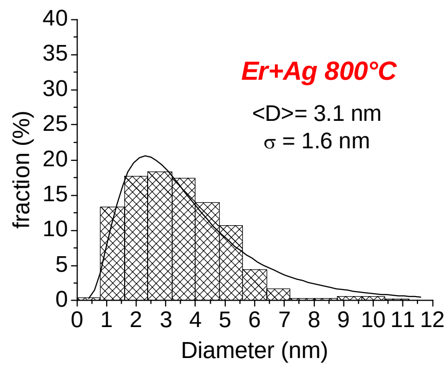


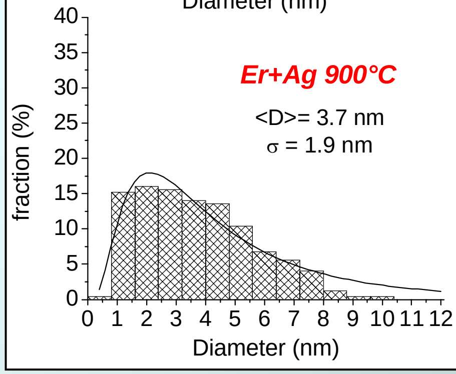


| Sample labels | <D> (nm) | σ (nm) |
|---|---|---|
| Er+Ag 600°C | 2.2 | 0.8 |
| Er+Ag 800°C | 3.1 | 1.6 |
| Er+Ag 900°C | 3.7 | 1.9 |

# Optical absorption measurements

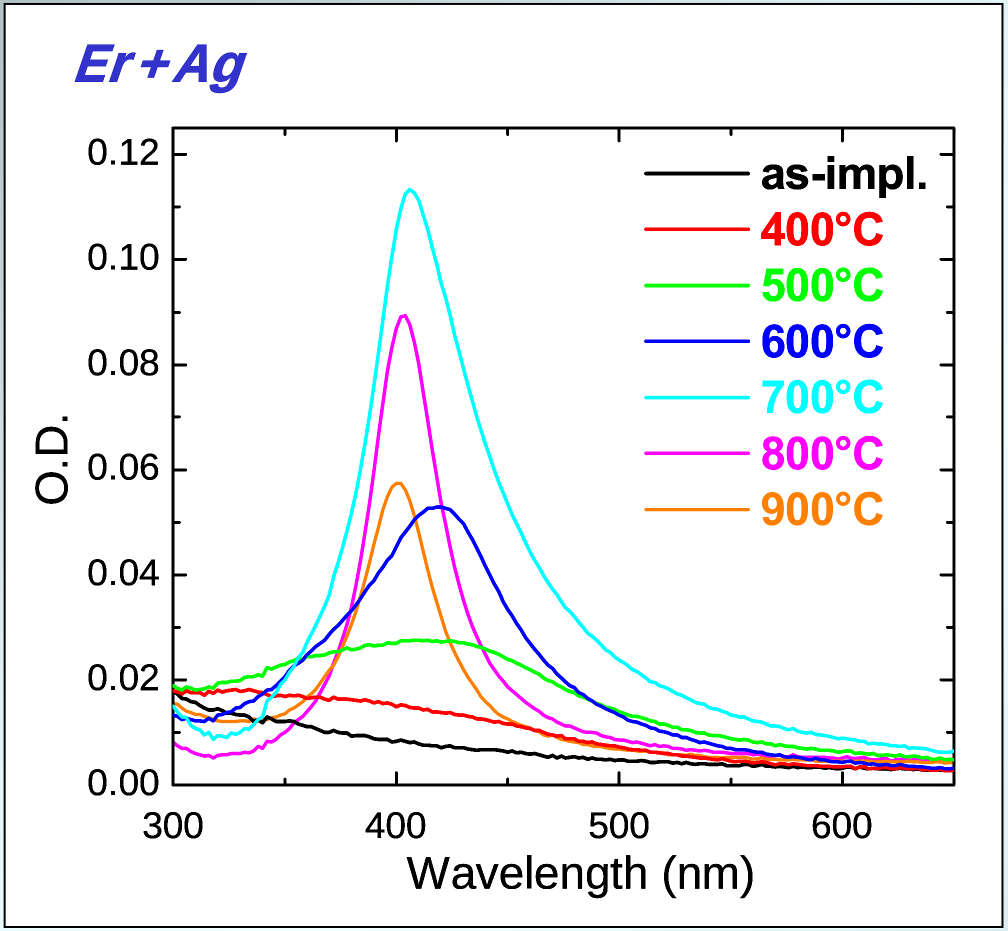


- ✓ Ag SPR band emerging as annealing T increases
- ✓ T>700°C, SPR intensity decreases

lower Ag content due to out-diffusion

## Er PL emission at 1.54 μm

# Er PL emission at 1.54 μm

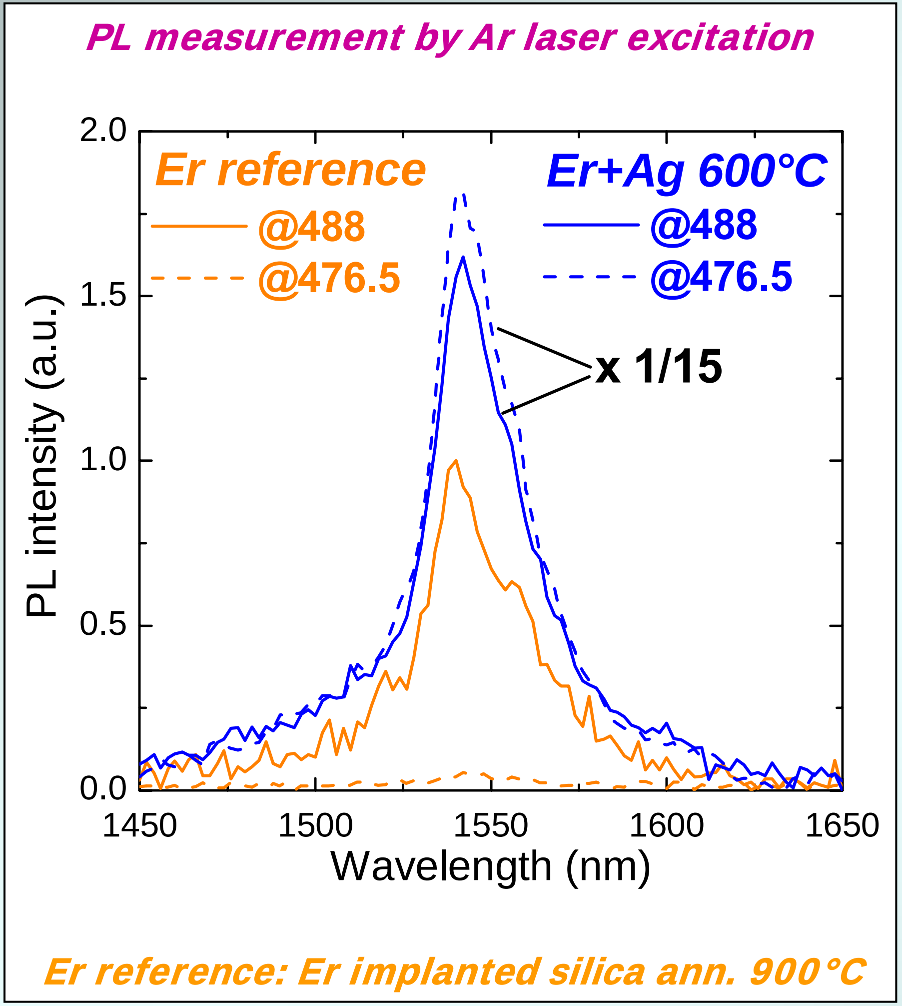


✓ Er reference:

★ PL emission at 1.54 μm only by resonant pumping (@488)

✓ Er+Ag 600°C:

★ increase of PL intensity with an enhancement factor of ~25

★ possibility of $Er^{3+}$ non-resonant excitation (@476.5)

$Er^{3+}$ sensitization through the opening of an Ag-mediated excitation path

# PLE measurements

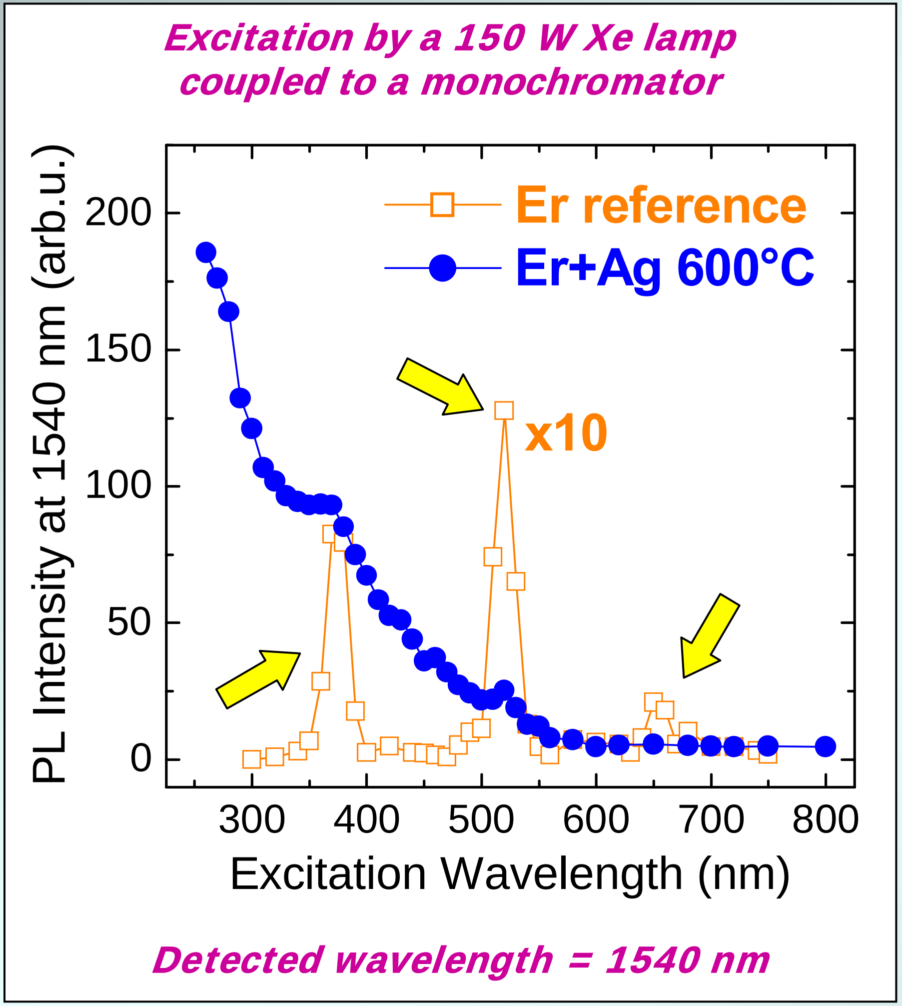


✓ Er reference:

★ 1.54 μm PL emission by direct $Er^{3+}$ light absorption

✓ Er+Ag 600°C:

★ $Er^{3+}$ can be stimulated over a continuous wavelength range

broadband pumping for $Er^{3+}$ excitation

# PLE vs OA spectra

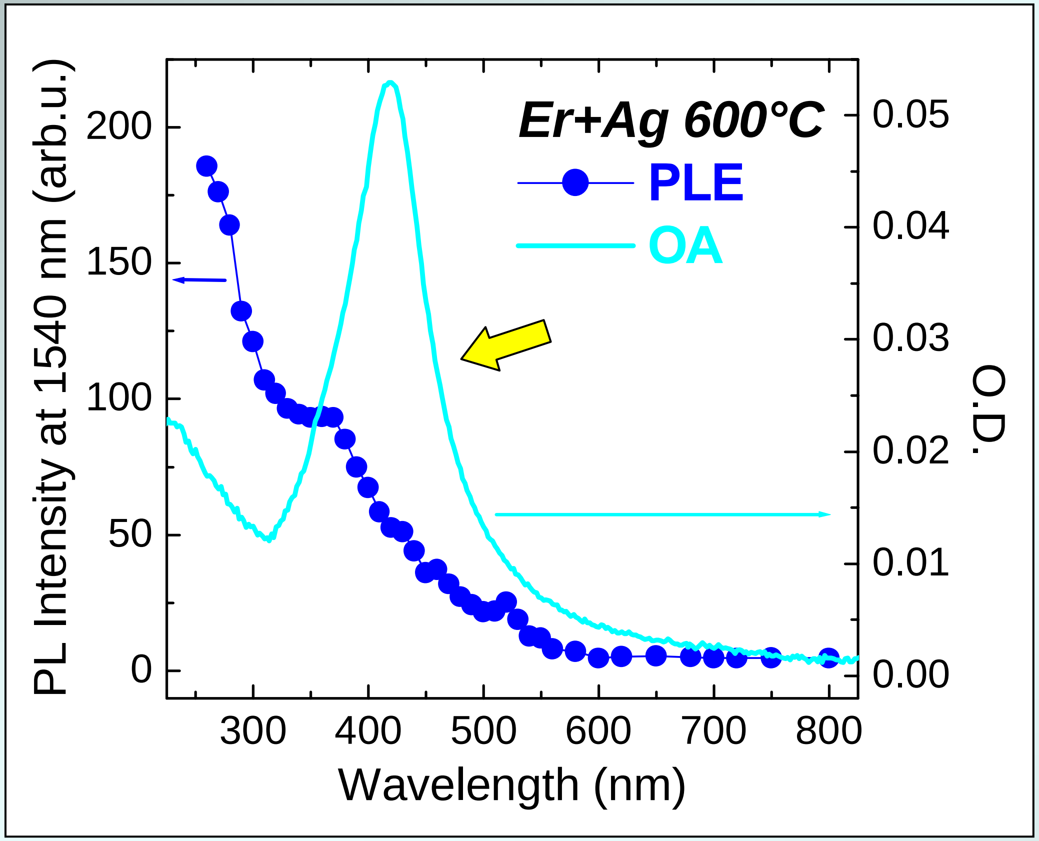


- ✓ PLE spectrum doesn't match SPR band

no effect due to the activation of Ag nanoparticle SPR

# PLE vs OA spectra

✓ Er implanted Ag-exchanged borosilicate glasses

***C. Strohhöfer et al., Appl. Phys. Lett. 81, 1414 (2002)***

Ag-related sensitizers (multimers, pairs of Ag ions/atoms) induce the enhancement of $Er^{3+}$ emission through light absorption and subsequent energy transfer process

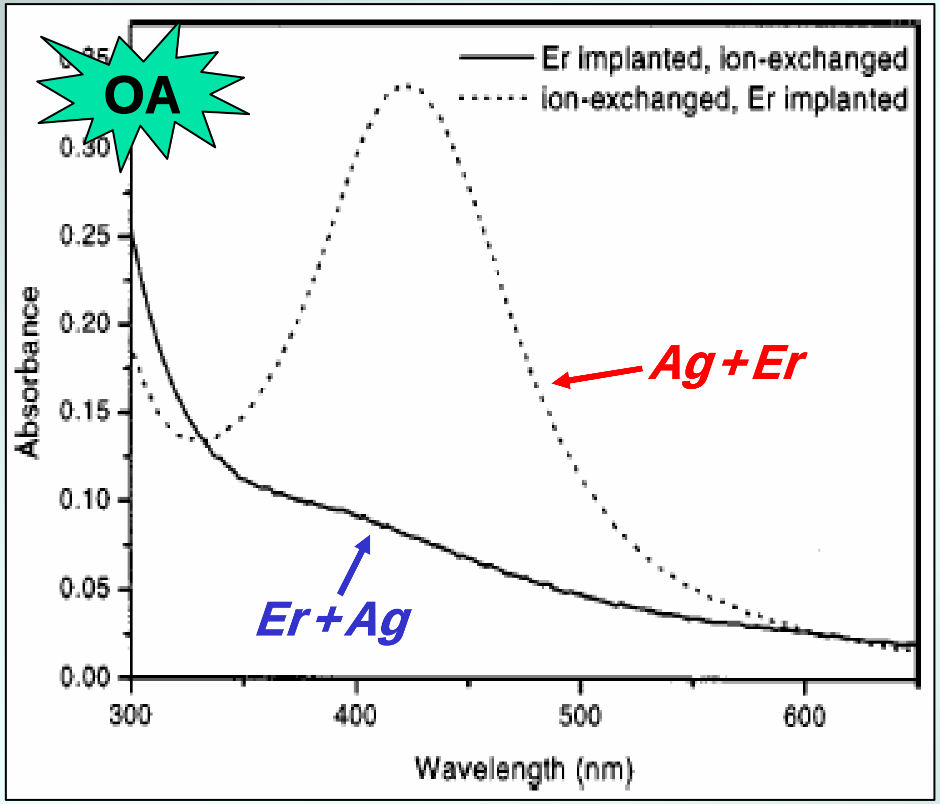


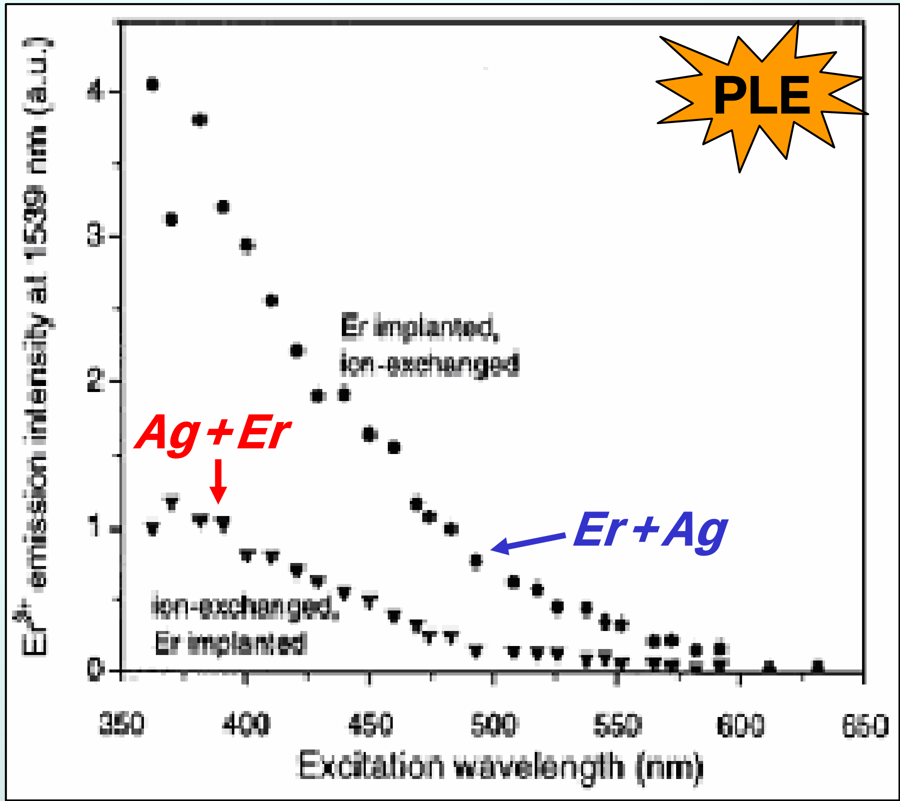

# PLE vs OA spectra

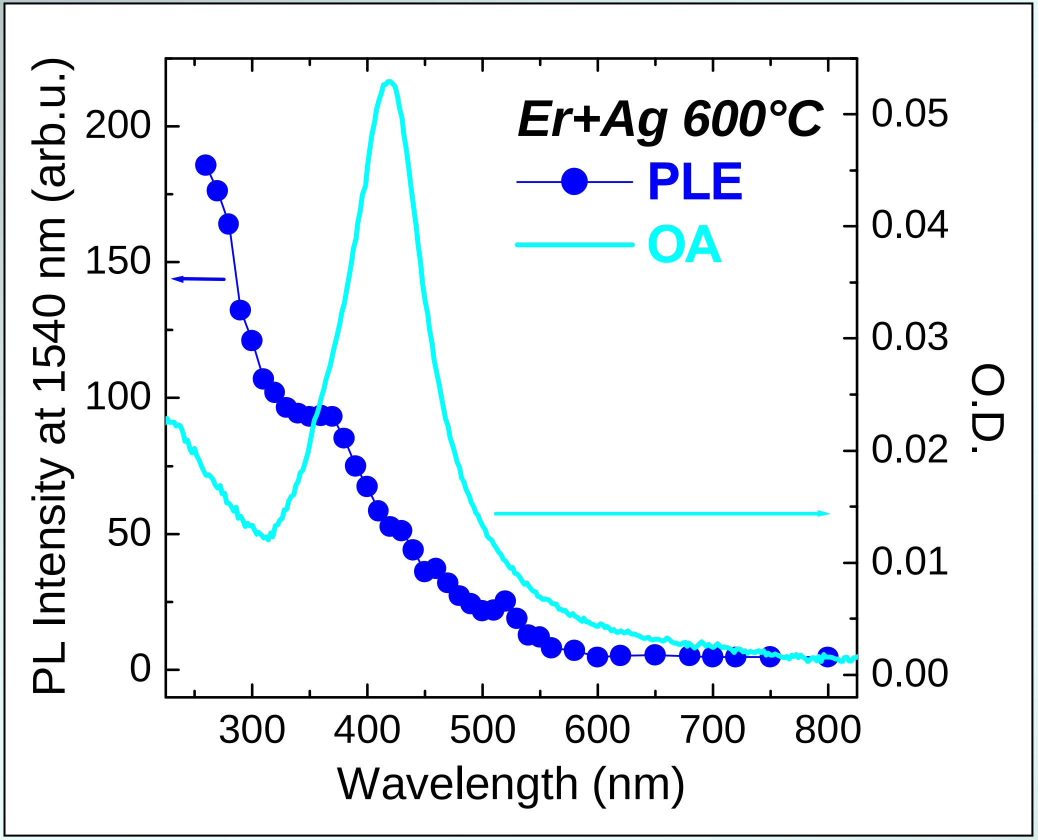


- ✓ PLE spectrum doesn't match SPR band

  ⬇

  no effect due to the activation of Ag nanoparticle SPR

- ✓ $Er^{3+}$ PL enhancement is due to energy transfer originating from light absorption by Ag-related sensitizers

# PL intensity vs annealing T

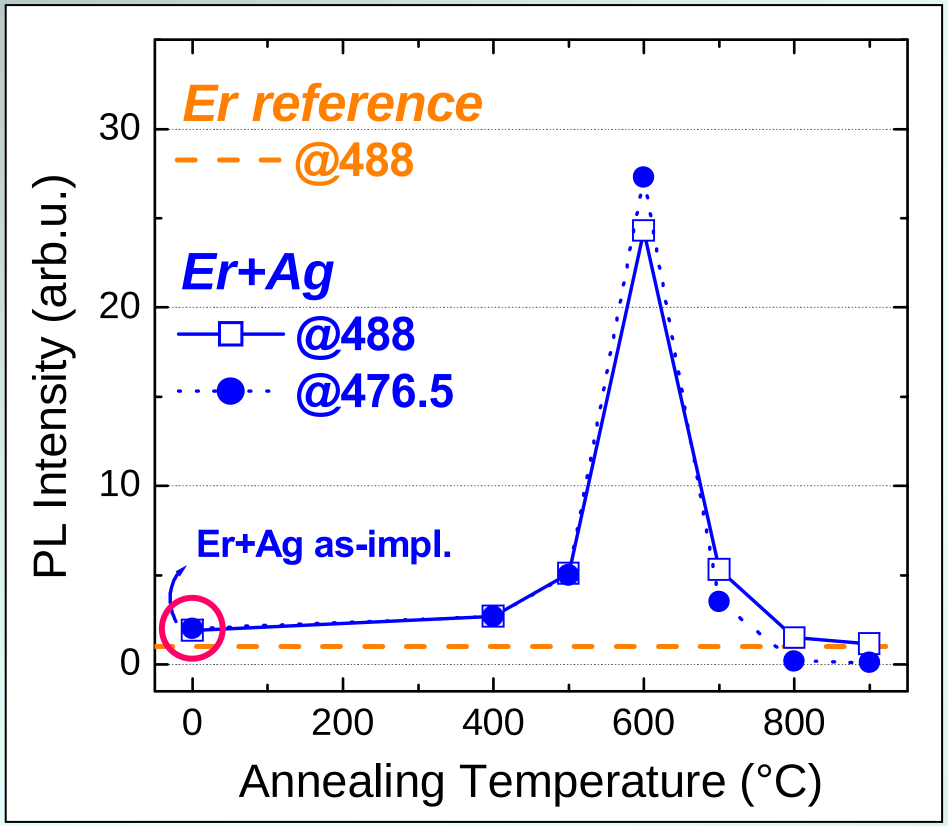


✓ After Ag implantation:

- ★ enhancement of PL emission
- ★ PL by non-resonant excitation

# PL intensity vs annealing T

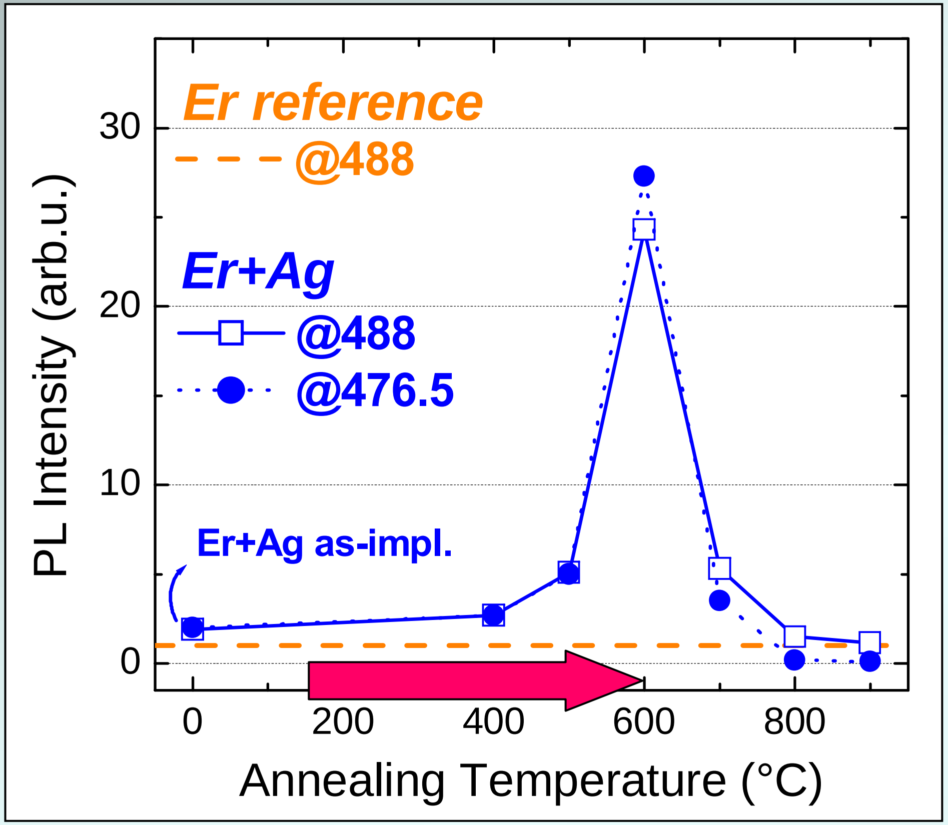


- After Ag implantation:
  - ★ enhancement of PL emission
  - ★ PL by non-resonant excitation

- PL intensity increases up to 600°C:
  - ★ further formation of sensitizers
  - ★ matrix recovery

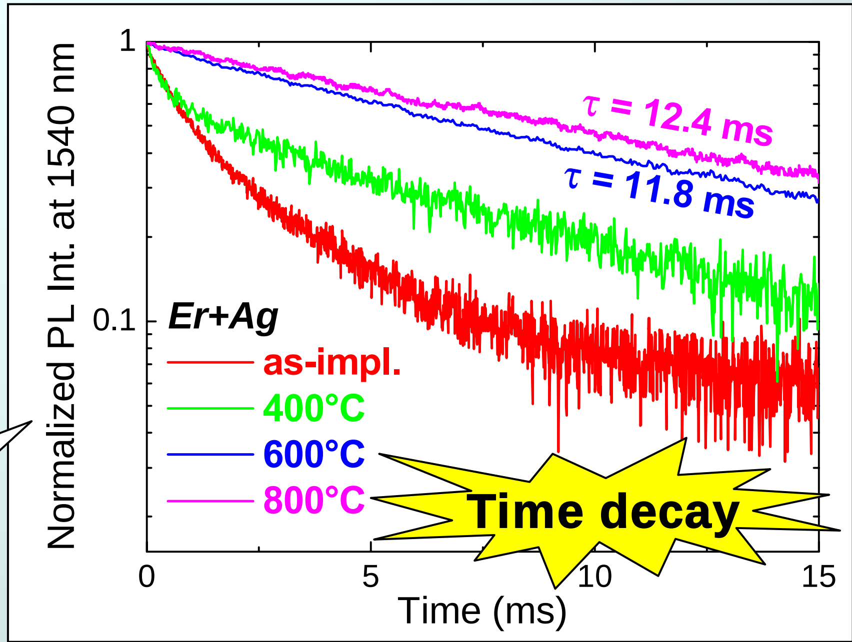


- Lifetime increases as annealing T rises
- Non-exponential behaviour for T<600°C

# PL intensity vs annealing T

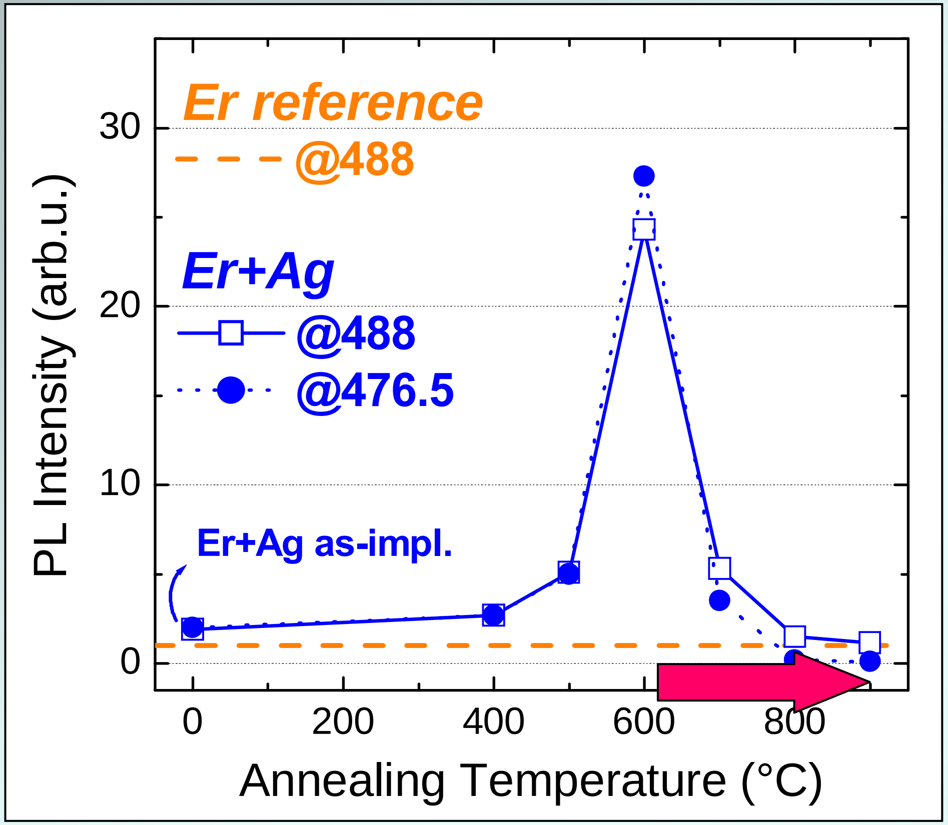


- ✓ After Ag implantation:
  - ★ enhancement of PL emission
  - ★ PL by non-resonant excitation
- ✓ PL intensity increases up to 600°C:
  - ★ further formation of sensitizers
  - ★ matrix recovery
- ✓ PL intensity decreases for T>600°C, no PL by @476.5 pump for T≥800°C:
  - ★ diminishing number of sensitizers
  - ★ decoupling between Er & sensitizers

# Ag-mediated effective cross section

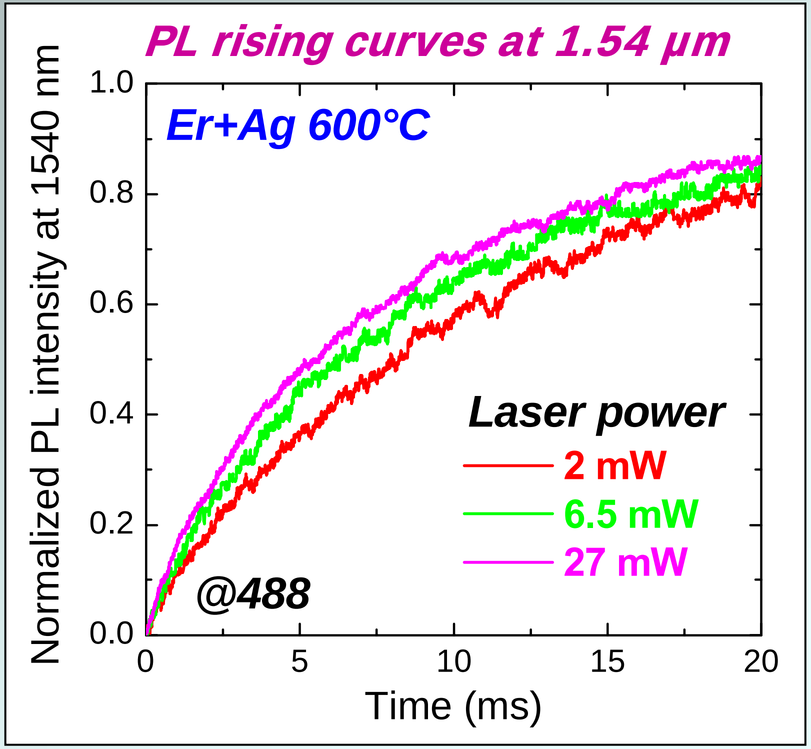


Dynamic conditions, laser turned on at *t=0*

$$I_{PL}(t) = I_{PL}^{0}\left\{1-\exp\left[-\left(\sigma_{eff}\phi+\frac{1}{\tau}\right)t\right]\right\}$$

$\tau_{on}$ = risetime $\quad \frac{1}{\tau_{on}} = \sigma_{eff}\phi + \frac{1}{\tau}$

***$\tau_{on}$ from PL rising curves***

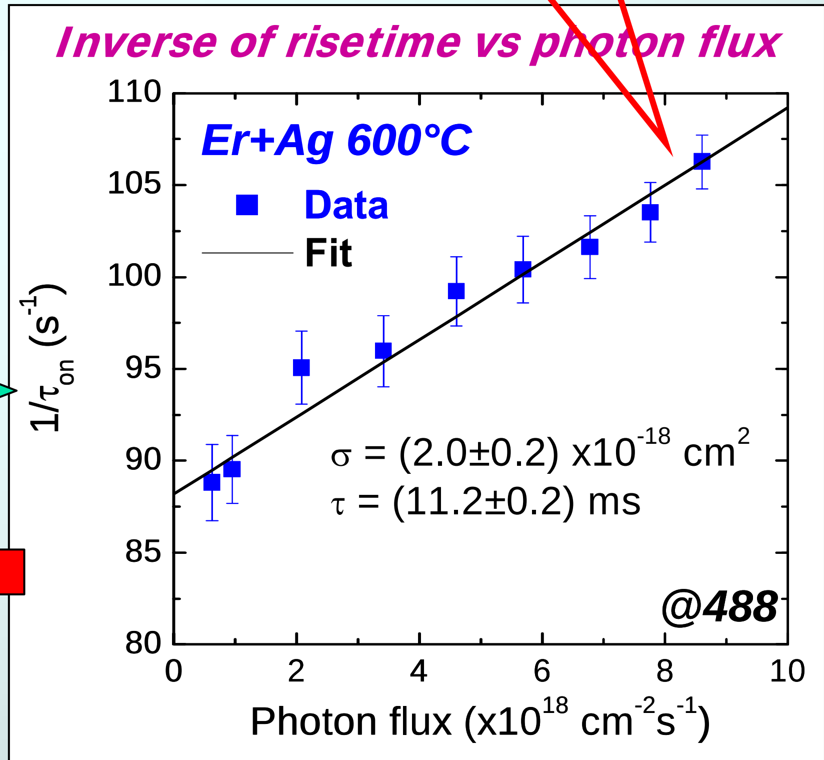


Effective cross section $\sigma_{eff}$
$(2.0\pm0.2)\times10^{-18}$ cm$^2$

($Er^{3+}$ direct $\sigma_{abs}$ ~ $10^{-20}$-$10^{-21}$ at 488 nm)

## Er and Au coimplantation in silica

# Er and Au coimplantation in silica

**Er**

| Fluence | Energy | Annealing (in $N_2$) |
|---|---|---|
| $6.8\times10^{14}$ at/cm$^2$ | 50+100+190 keV | 900°C, 1h |

**+**

**Au**

| Fluence | Energy | Annealing (in $N_2$) |
|---|---|---|
| $6.1\times10^{15}$ at/cm$^2$ | 60+110+190 keV | 400→900°C, 1h |

**Thermal treatment:**

✓ Matrix recovery

✓ Activation of metal migration and aggregation processes

★ *Structural and optical measurements*

Evolution of Au aggregation

★ *PL investigation*

Er luminescence behaviour

# Compositional characterization

**Er**

| Fluence | Energy | Annealing (in $N_2$) |
|---|---|---|
| $6.8\times10^{14}$ at/cm$^2$ | 50+100+190 keV | 900°C, 1h |

**+**

**Au**

| Fluence | Energy | Annealing (in $N_2$) |
|---|---|---|
| $6.1\times10^{15}$ at/cm$^2$ | 60+110+190 keV | 400→900°C, 1h |

***SIMS + RBS compositional analysis***

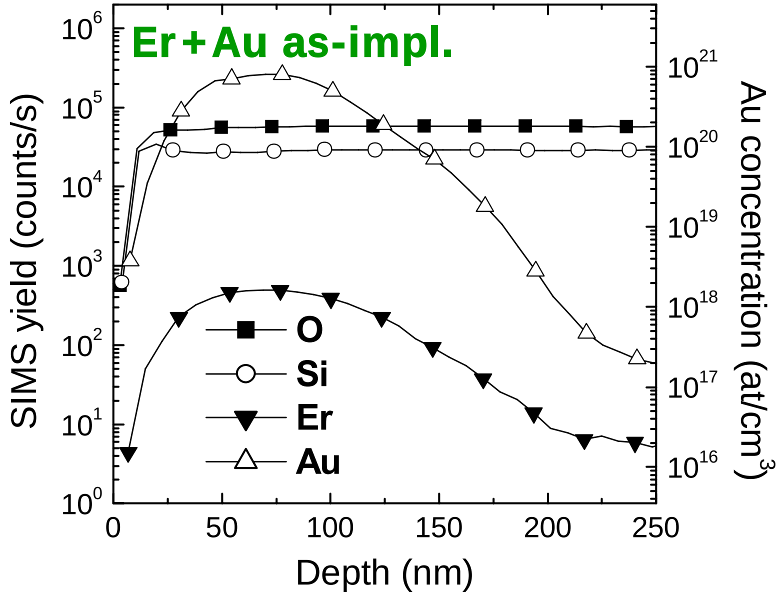


- ✓ Au and Er profiles overlapped after implant and also after annealing
- ✓ Au conc. and dose ~ constant after annealing

| | *conc. ($Au^+/cm^3$)* | *dose ($Au^+/cm^2$)* |
|---|---|---|
| **as-impl.** | $8.2\times10^{20}$ | $6.1\times10^{15}$ |
| **ann. 800°C** | $9.4\times10^{20}$ | $5.8\times10^{15}$ |

# TEM analysis

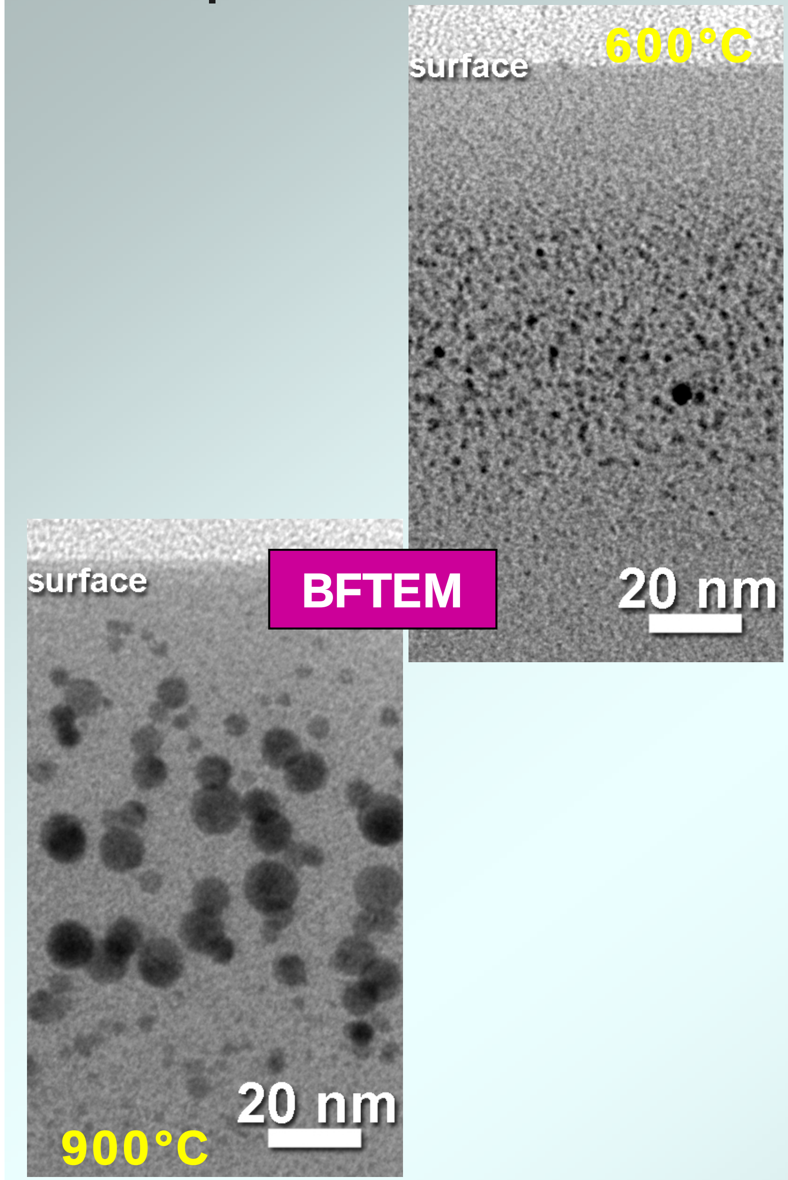


- ✓ Precipitation of Au clusters
- ✓ Spherical clusters in a ~80-100 nm region located at a depth of ~70 nm
- ✓ Cluster size increases with the annealing T (manifest <D> increase at T=900°C)

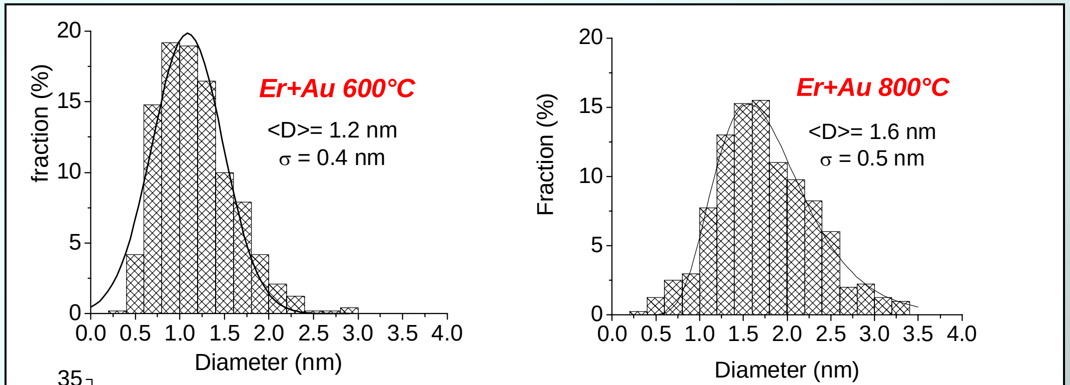


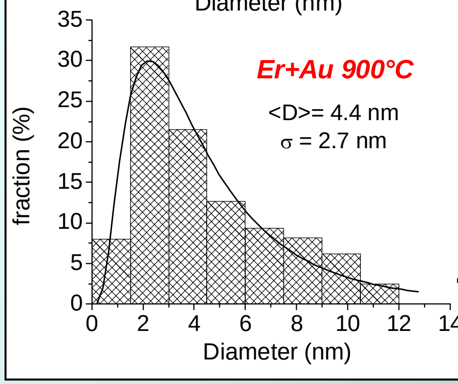


| Sample labels | <D> (nm) | σ (nm) |
|---|---|---|
| Er+Au 600°C | 1.2 | 0.4 |
| Er+Au 800°C | 1.6 | 0.5 |
| Er+Au 900°C | 4.4 | 2.7 |

# Local environment around Au

**EXAFS** at the Au $L_{III}$-edge

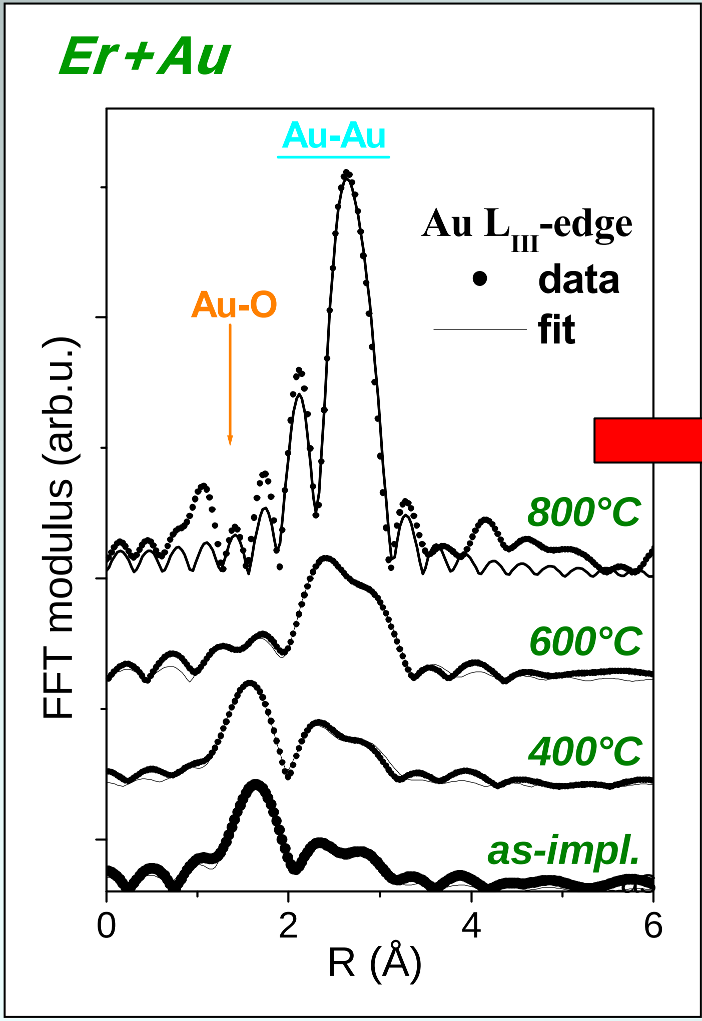


✓ Presence of Au-O coordination

| Sample label | Coord. | R (Å) | N | $\sigma^2$ ($\times 10^{-4}$ Å$^2$) |
|---|---|---|---|---|
| Er+Au as-impl. | Au-O | 2.02±0.02 | 1.1±0.1 | 51±30% |
| | Au-Au | 2.73±0.02 | 0.8±0.1 | 56±30% |
| Er+Au 400°C | Au-O | 1.96±0.02 | 1.3±0.1 | 51±30% |
| | Au-Au | 2.74±0.02 | 1.2±0.1 | 56±30% |
| Er+Au 600°C | Au-O | 1.94±0.02 | 0.5±0.1 | 51±30% |
| | Au-Au | 2.79±0.02 | 3.7±0.1 | 75±30% |
| Er+Au 800°C | Au-Au | 2.81±0.02 | 6.7±0.1 | 75±30% |
| Au reference | Au-Au | 2.88±0.02 | 12 | - |

✓ Au-Au coordination: precipitation of Au aggregates

Larger mean size as annealing T rises up
- ★ *R* tends to $R_{bulk}$
- ★ *N* increasing

# Optical absorption measurements

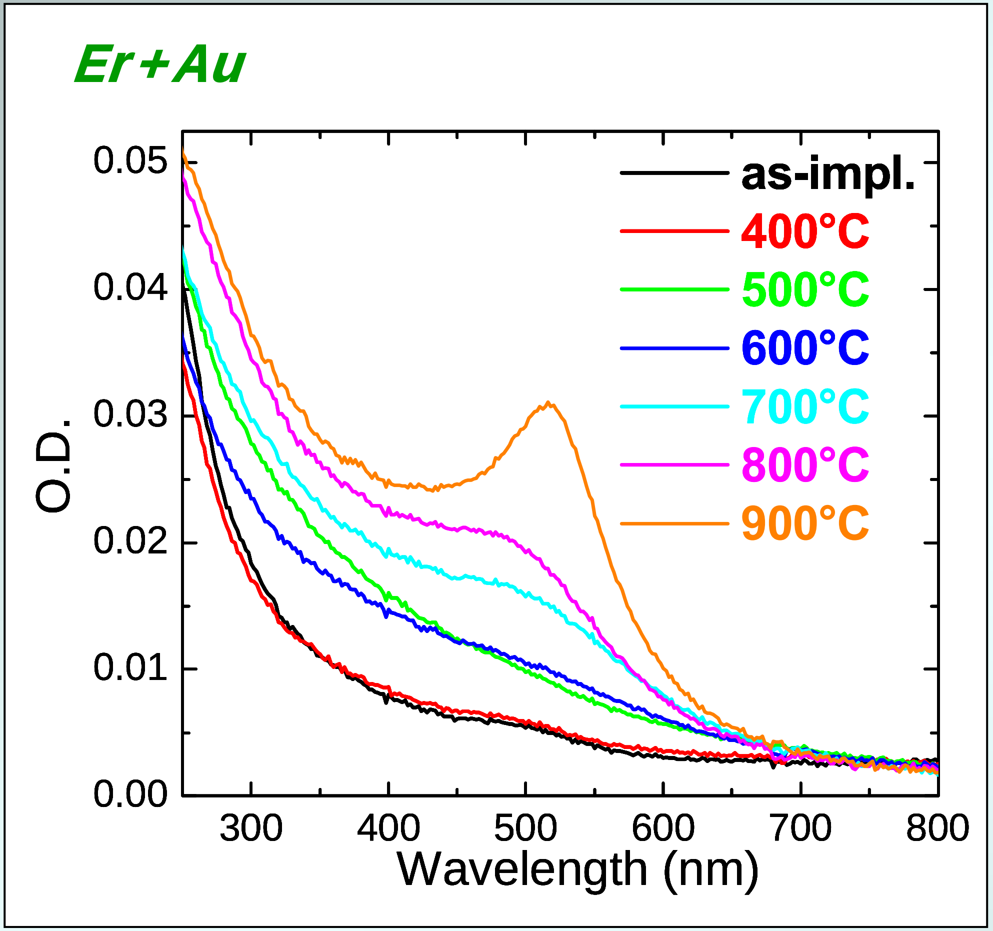


- ✓ After metal incorporation, OA profile increasing towards the UV

Au interband transitions
(edge at ~1.7 eV)

- ✓ Ag SPR band emerging as annealing T increases

## Er PL emission at 1.54 μm

# Er PL emission at 1.54 μm

*PL measurement by Ar laser excitation*

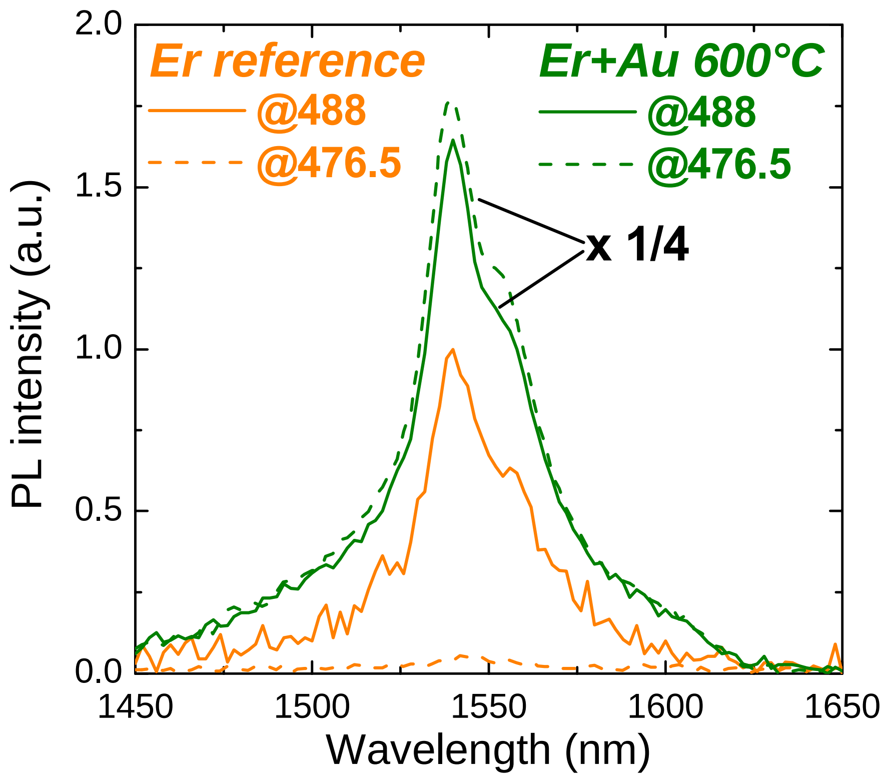


*Er reference: Er implanted silica ann. 900°C*

✓ Er reference:

★ PL emission at 1.54 μm only by resonant pumping (@488)

✓ Er+Au 600°C:

★ increase of PL intensity with an enhancement factor of ~7

★ possibility of $Er^{3+}$ non-resonant excitation (@476.5)

$Er^{3+}$ sensitization through the opening of an Au-mediated excitation path

# PL intensity vs annealing T

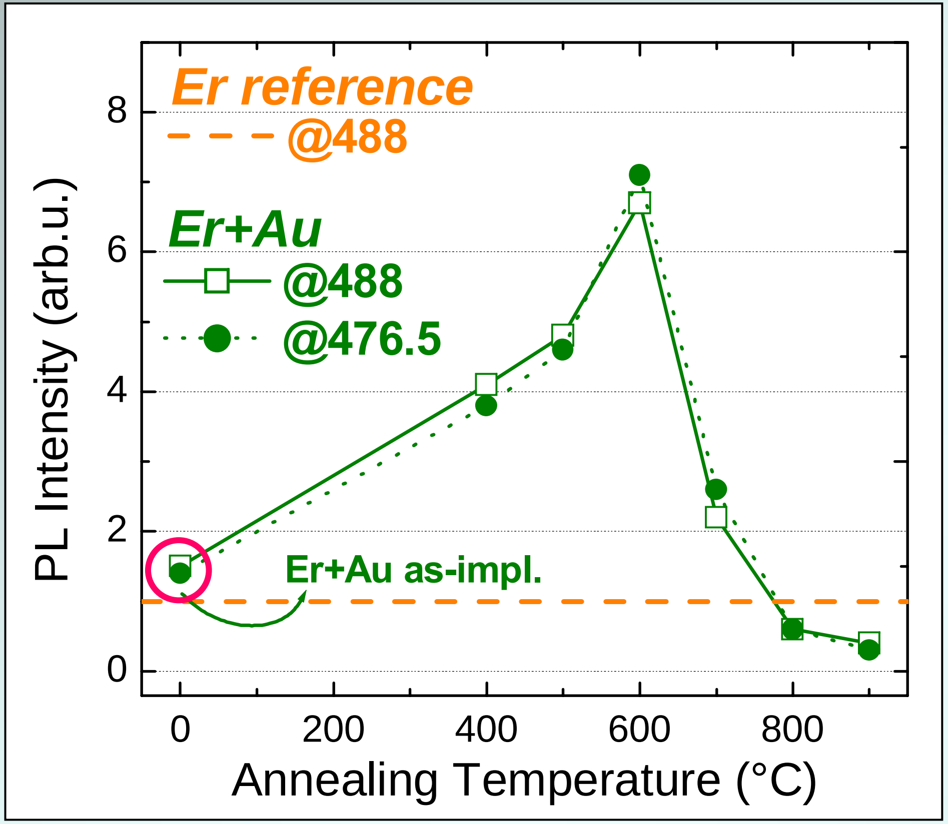


✓ After Au implantation:

- ★ enhancement of PL emission
- ★ PL by non-resonant excitation

# PL intensity vs annealing T

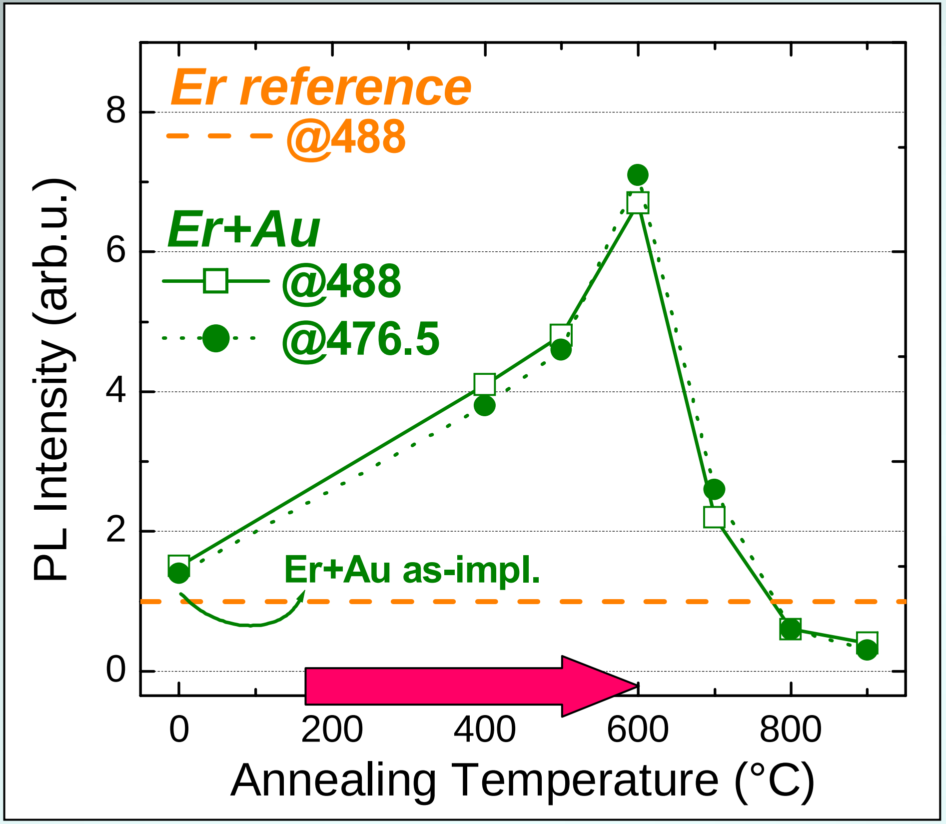


- ✓ After Au implantation:
  - ★ enhancement of PL emission
  - ★ PL by non-resonant excitation
- ✓ PL intensity increases up to 600°C:
  - ★ further formation of sensitizers
  - ★ matrix recovery

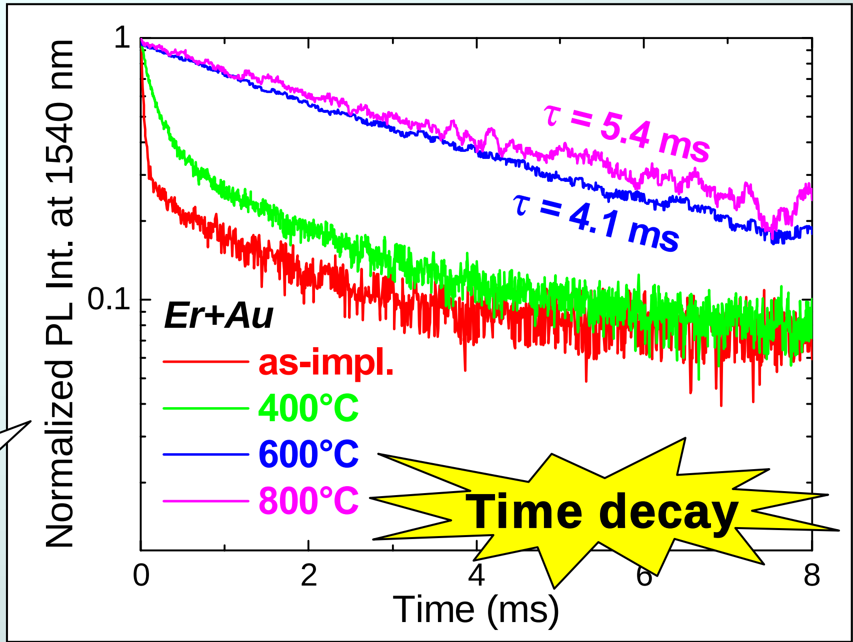


- ➢ Lifetime increases as annealing T rises
- ➢ Non-exponential behaviour for T<600°C

# PL intensity vs annealing T

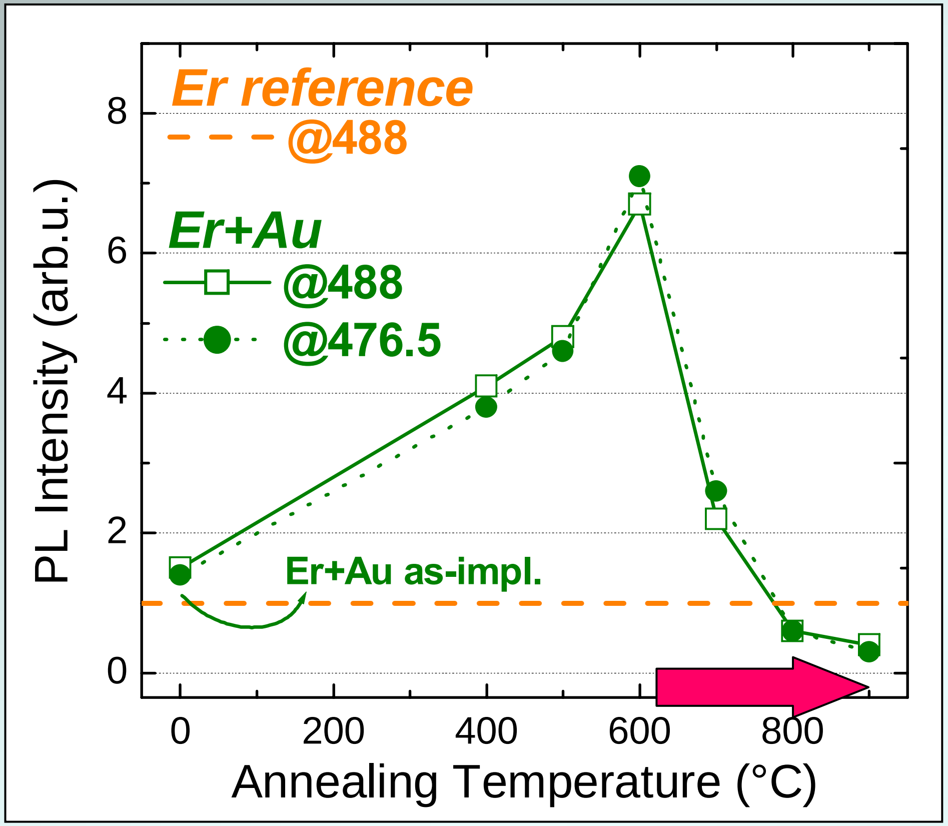


✓ After Au implantation:

★ enhancement of PL emission
★ PL by non-resonant excitation

✓ PL intensity increases up to 600°C:

★ further formation of sensitizers
★ matrix recovery

✓ PL intensity decreases for T>600°C:

★ diminishing number of sensitizers
★ decoupling between Er & sensitizers

# Au-mediated effective cross section

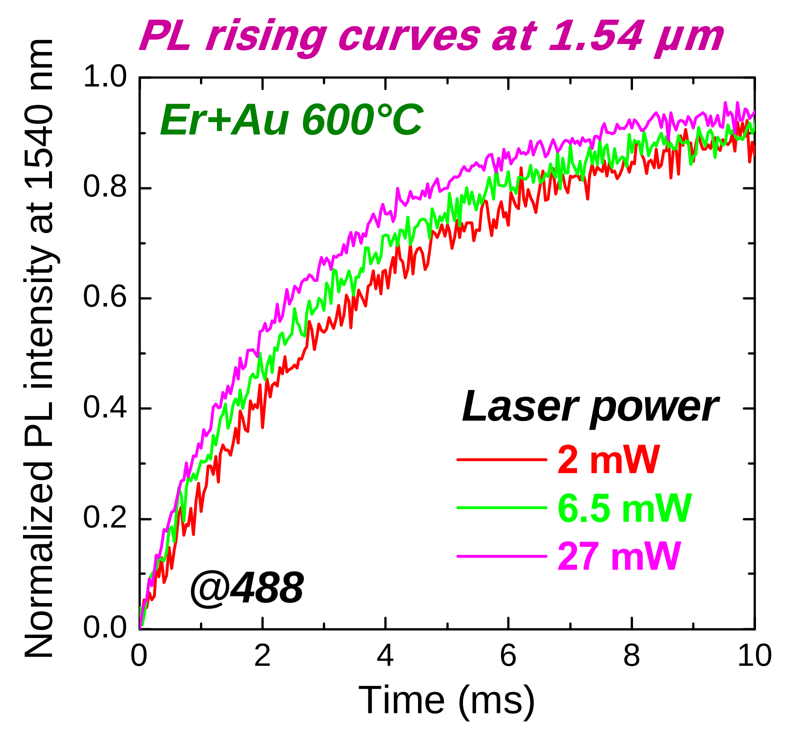


Dynamic conditions, laser turned on at $t=0$

$$I_{PL}(t) = I_{PL}^{0}\left\{1-\exp\left[-\left(\sigma_{eff}\phi+\frac{1}{\tau}\right)t\right]\right\}$$

$\tau_{on}$ = risetime $\quad \dfrac{1}{\tau_{on}} = \sigma_{eff}\phi + \dfrac{1}{\tau}$

$\tau_{on}$ **from PL rising curves**

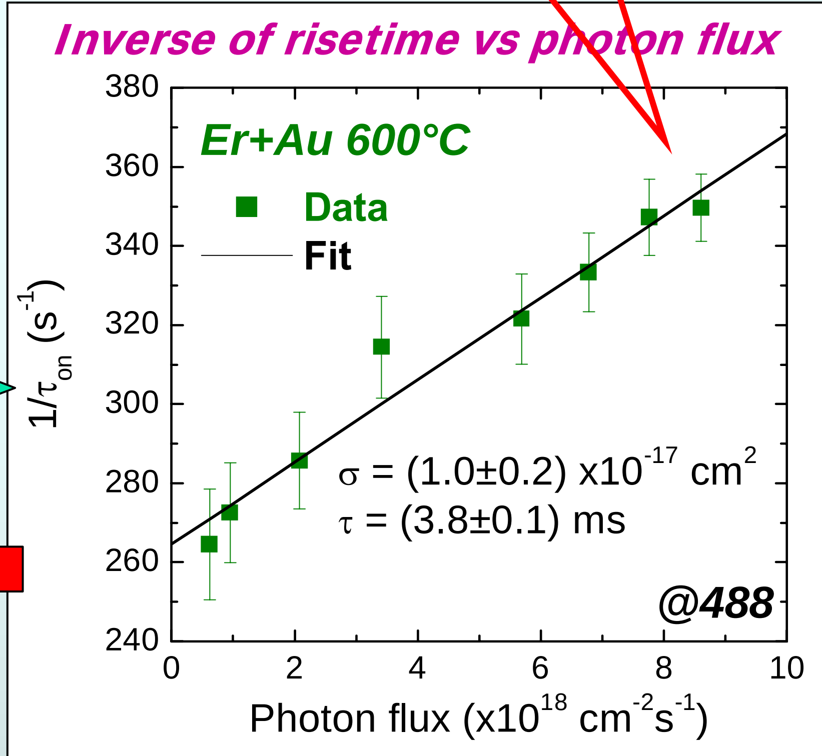


Effective cross section $\sigma_{eff}$
$(1.0\pm0.2)\times10^{-17}$ cm$^2$

($Er^{3+}$ direct $\sigma_{abs} \sim 10^{-20}$-$10^{-21}$ at 488 nm)

# PLE measurements

*Excitation by a 150 W Xe lamp coupled to a monochromator*

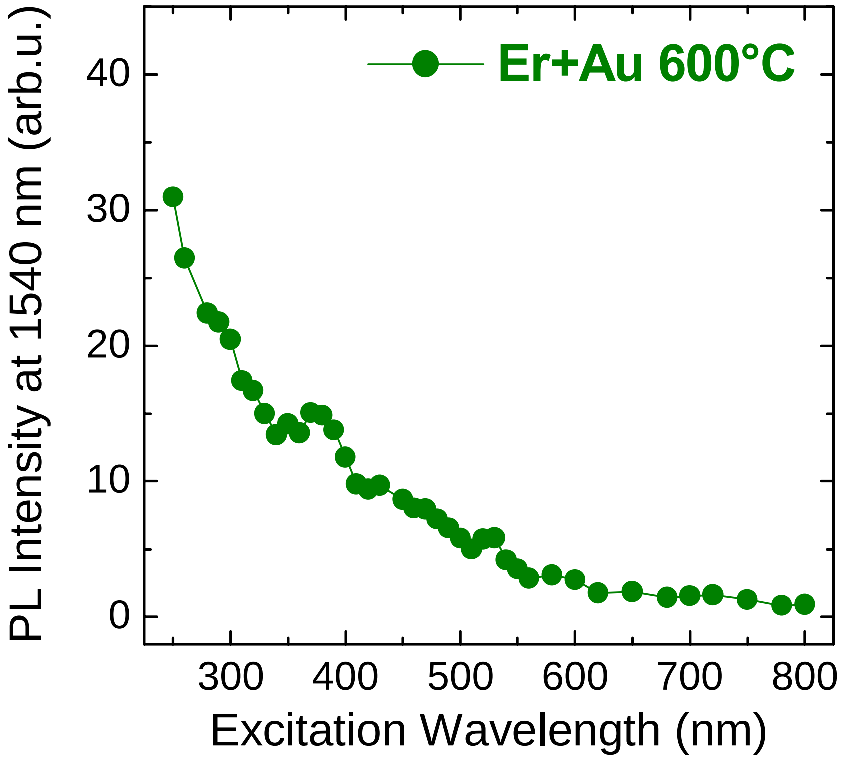


*Detected wavelength = 1540 nm*

✓ Er+Au 600°C:

★ $Er^{3+}$ can be stimulated over a continuous wavelength range

⬇

broadband pumping for $Er^{3+}$ excitation

# PLE vs OA spectra

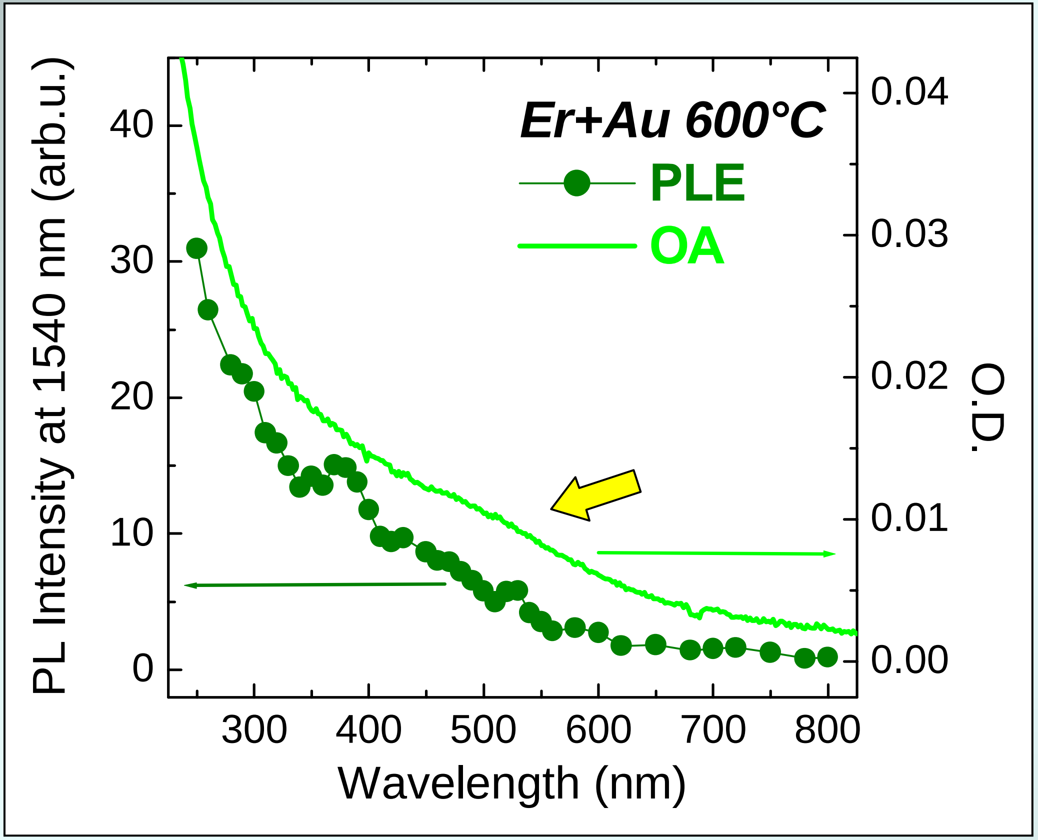


✓ Er+Au 600°C:

★ $Er^{3+}$ can be stimulated over a continuous wavelength range

broadband pumping for $Er^{3+}$ excitation

✓ PLE profile almost matches OA spectrum, except for SPR band:

★ no effect due to the activation of Au nanoparticle SPR

★ energy transfer originating from light absorption by Au-related sensitizers

★ sensitizers optically activated by Au interband absorption

# Au luminescence properties

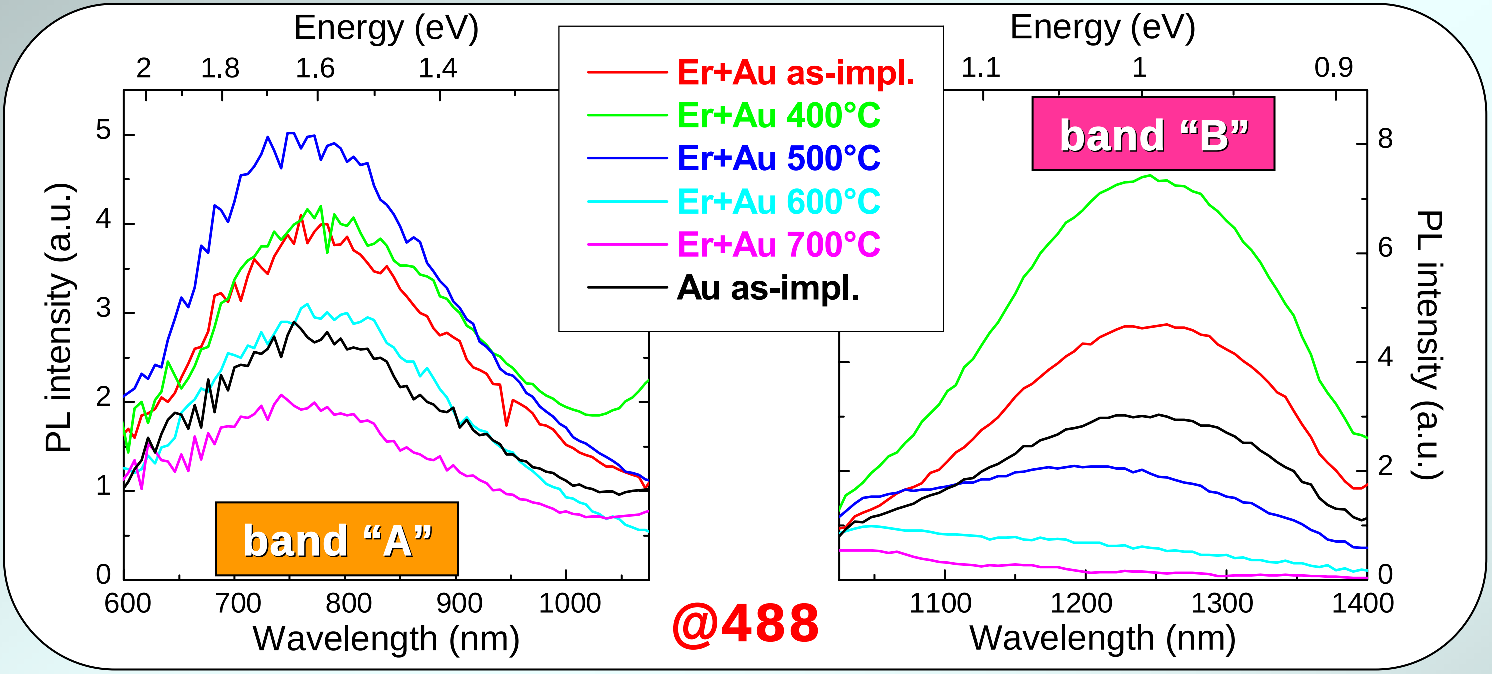


- ✓ Appearance of two PL emission bands in the red – near-IR
- ✓ Au as-impl. shows the same luminescence activity
- ✓ PL bands already manifest after metal implantation

# Au luminescence properties

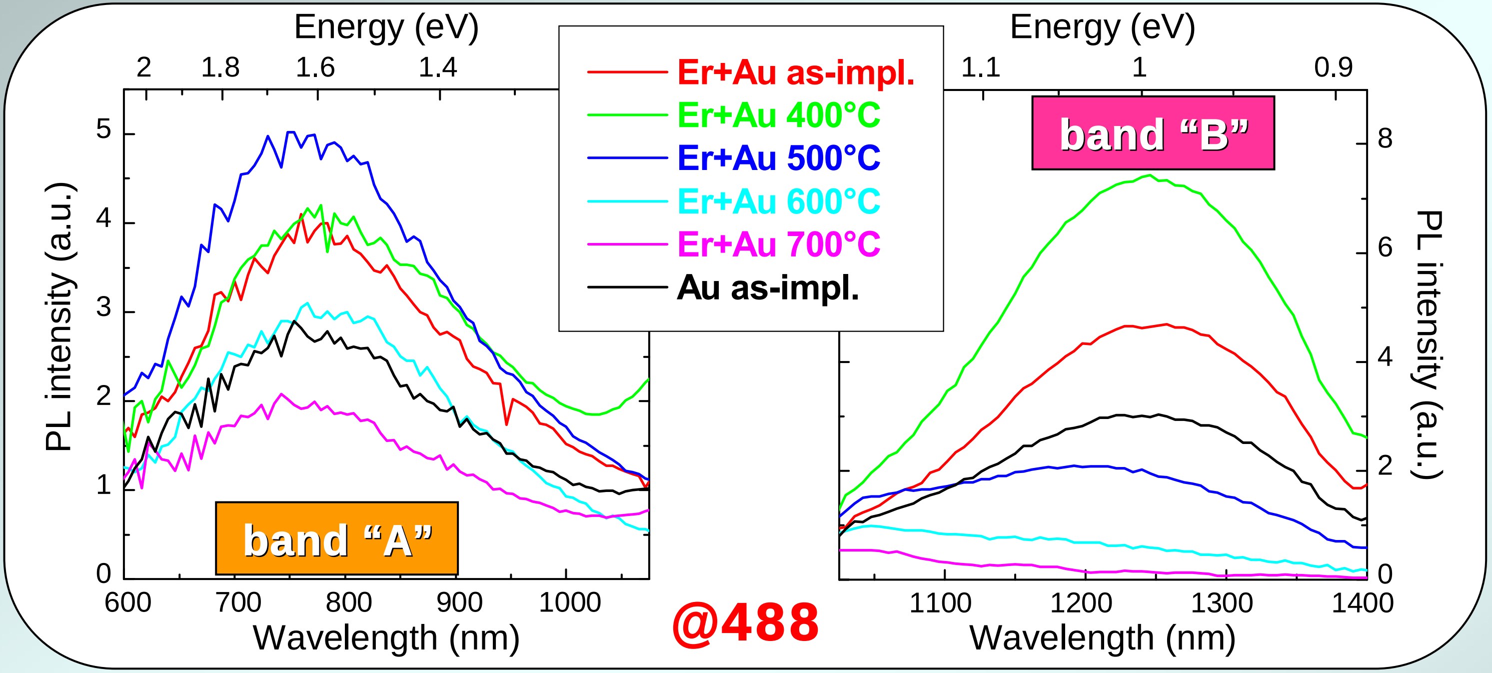


- ✓ PL intensity vs annealing T:
  - ★ band “A” PL maximum at 500°C, intensity decreases for T>500°C
  - ★ band “B” PL maximum at 400°C, intensity ~0 at 600°C

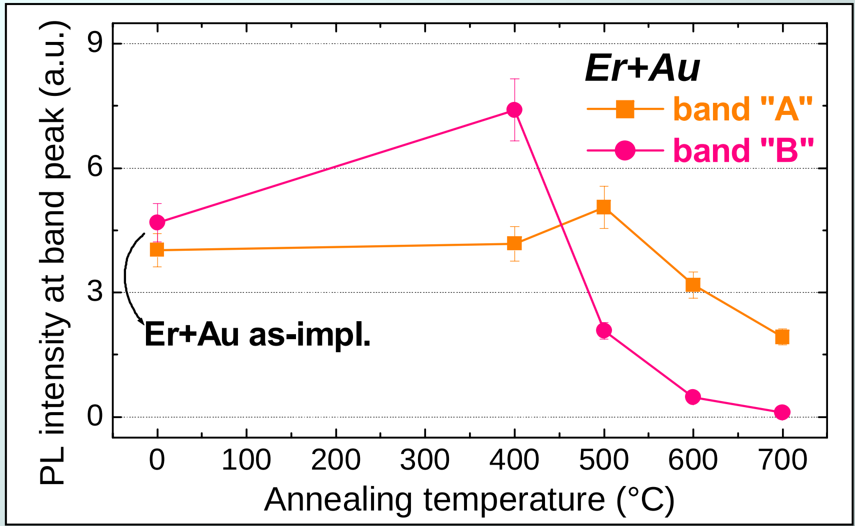

# Au luminescence properties

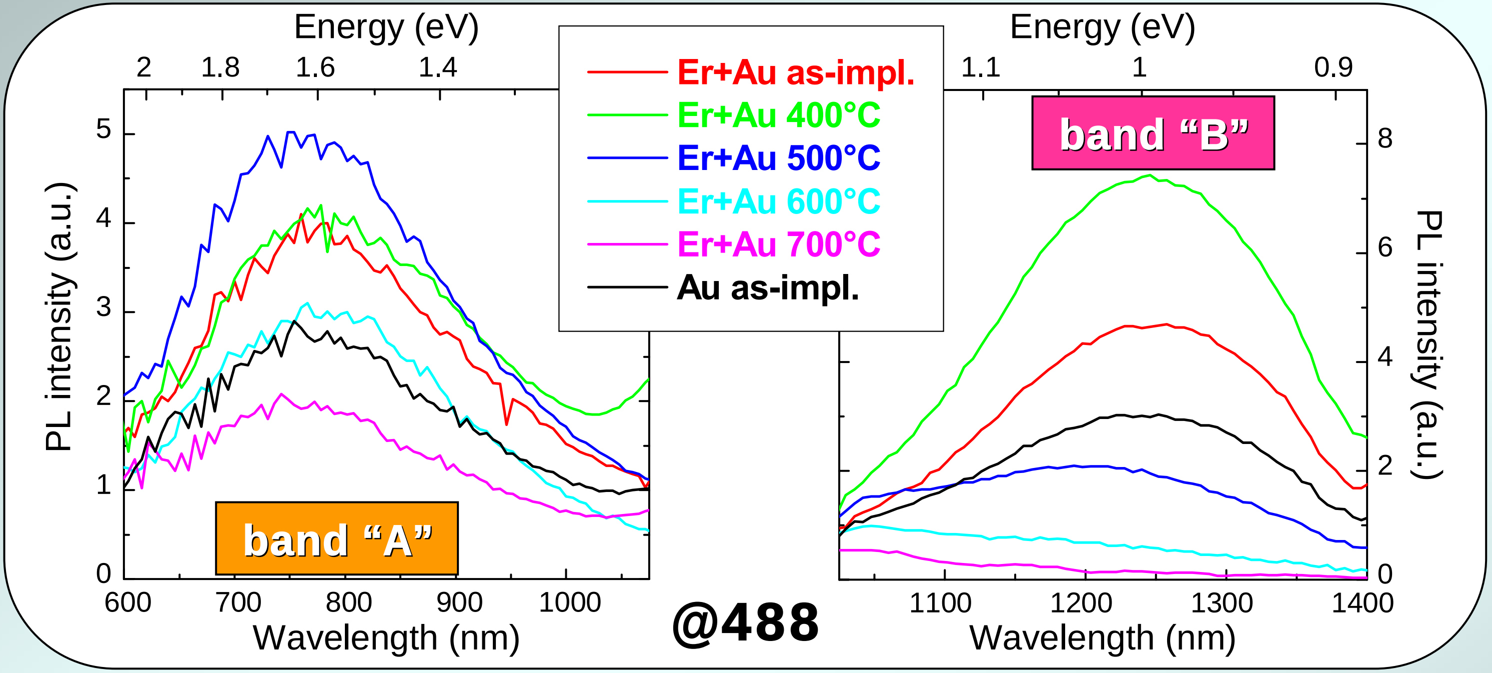


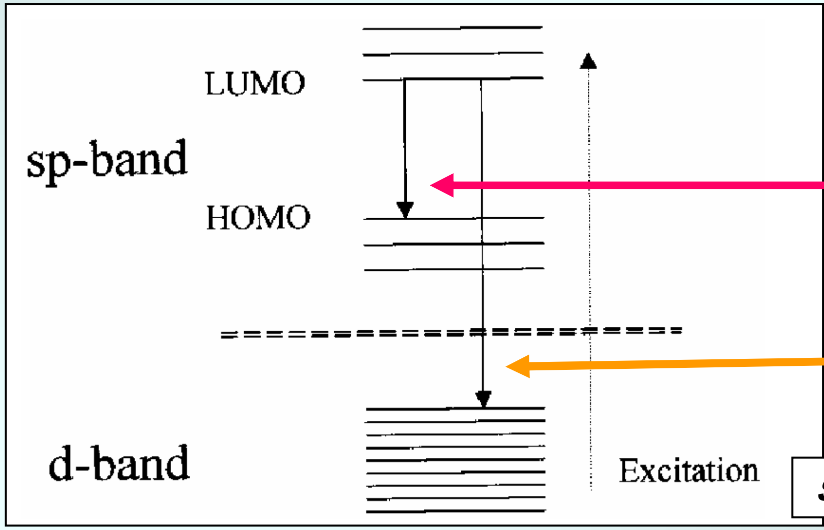


✓ Mechanism originating PL bands:

★ band "B" linked to intraband transition (observation of an onset in OA spectra)

★ band "A" linked to interband transition

*S. Link et al., J. Phys. Chem. B 106, 3410 (2002)*

## Ag-exchanged Er doped sol-gel films

# Ag-exchanged Er doped sol-gel films: synthesis

**Deposition of multilayer sol-gel films by dipping**

$SiO_2$-$Al_2O_3$-$Na_2O$ glass (3/6/9 mol% $Na_2O$)
0.5% Er (~$10^{20}$ ions/cm$^3$)

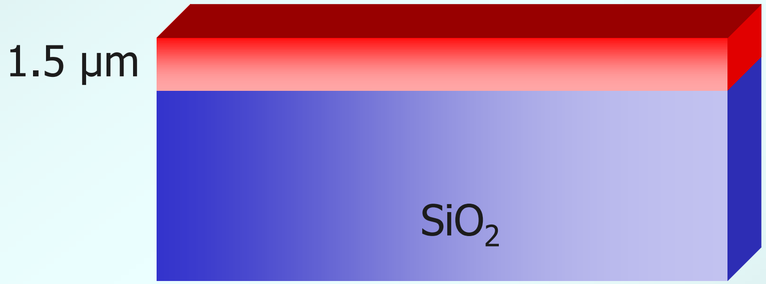


**$Ag^+$-$Na^+$ ion exchange**

molten salt bath:
1 or 12 mol% $AgNO_3$ in $NaNO_3$
(0.8 or 2.5·$10^{21}$ $Ag^+$/cm$^3$ in the film)

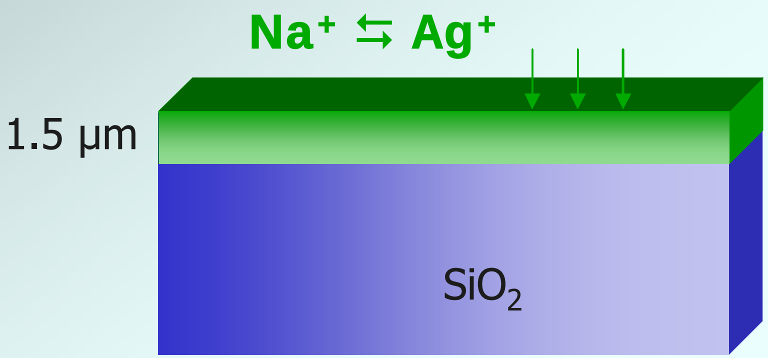


**Thermal annealing**
(3h, 5h in $N_2$ at 500 °C)

**$He^+$ irradiation**
(1 or 6·$10^{17}$ ions/cm$^2$)

Ag pairs
Ag multimers
Ag clusters

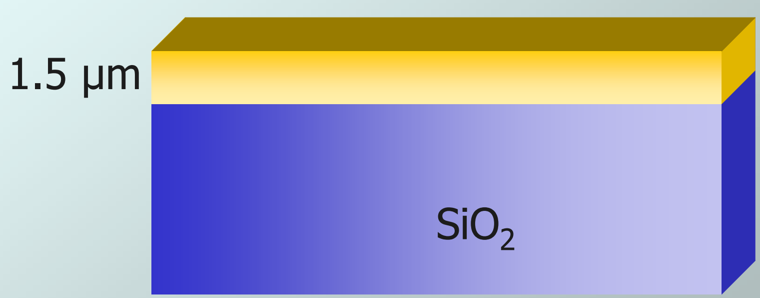

# Effect of glass composition on 1.54 μm PL band shape

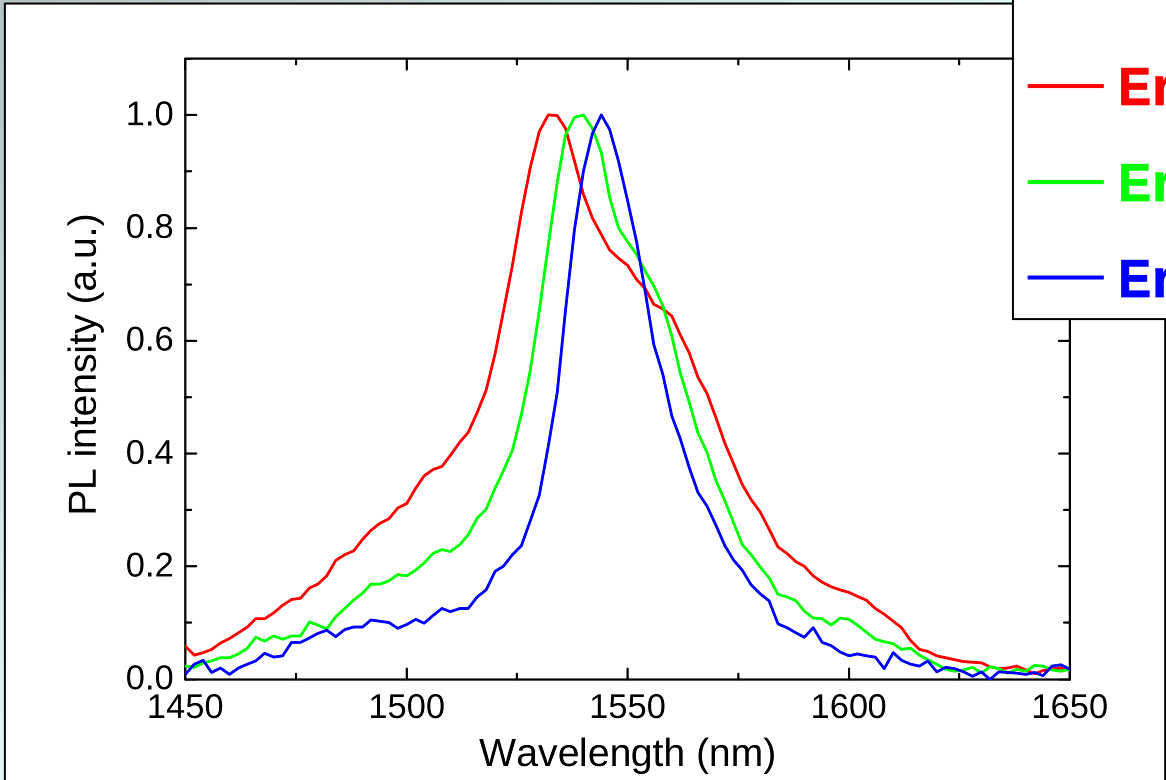


*Excitation wavelength = 488 nm*

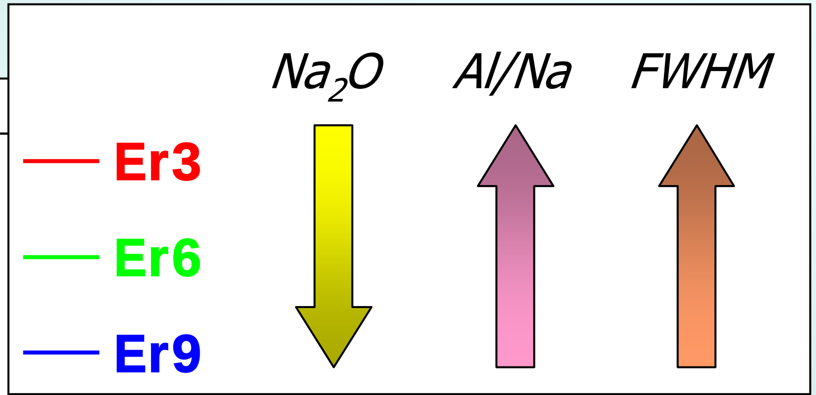


Al/Na ratio (>1) increase

More structural units in the glass

Larger distribution of sites for $Er^{3+}$

Broadening of $Er^{3+}$ PL emission at 1.54 μm

Technological remark: bandwidth tunability acting on the glass composition

# Er PL emission at 1.54 µm: Er doped sol-gel

| Sample label | PL int. @488 | PL int. @476.5 | Lifetime (ms) |
|---|---|---|---|
| Er9 | 1.0 | ~0 | 11.0 |
| Er9Ag | 0.5 | ~0 | 7.7 |
| Er9Ag-3h500 | 3.0 | 2.9 | 8.0 |
| Er9Ag-5h500 | 3.2 | 3.4 | 8.2 |
| Er9Ag-3h500 1He | 6.1 | 6.5 | 7.2 |
| Er9Ag-3h500 6He | 0.9 | 0.9 | 5.4 |

***PL int.** referred to the normalized **Er9** resonant emision*

**Er9**

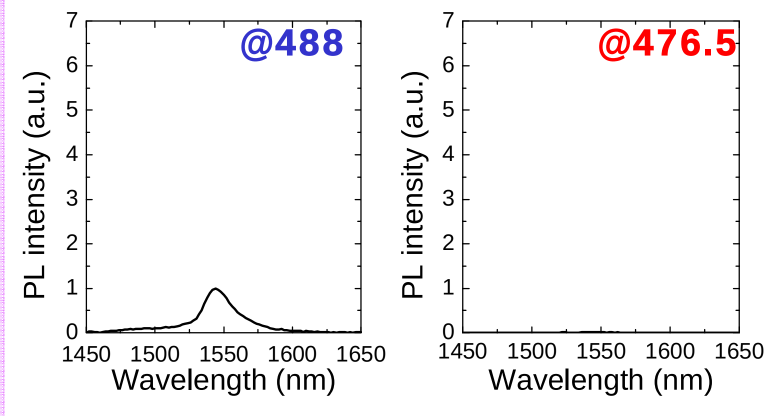


**Sol-gel** (9 mol% $Na_2O$)

✓ No sensitizing elements

☺ No energy transfer

☹ Small cross section

# Er PL emission at 1.54 μm: as-exchanged samples

| Sample label | PL int. @488 | PL int. @476.5 | Lifetime (ms) |
|---|---|---|---|
| Er9 | 1.0 | ~0 | 11.0 |
| Er9Ag | 0.5 | ~0 | 7.7 |
| Er9Ag-3h500 | 3.0 | 2.9 | 8.0 |
| Er9Ag-5h500 | 3.2 | 3.4 | 8.2 |
| Er9Ag-3h500 1He | 6.1 | 6.5 | 7.2 |
| Er9Ag-3h500 6He | 0.9 | 0.9 | 5.4 |

***PL int.*** *referred to the normalized* ***Er9*** *resonant emision*

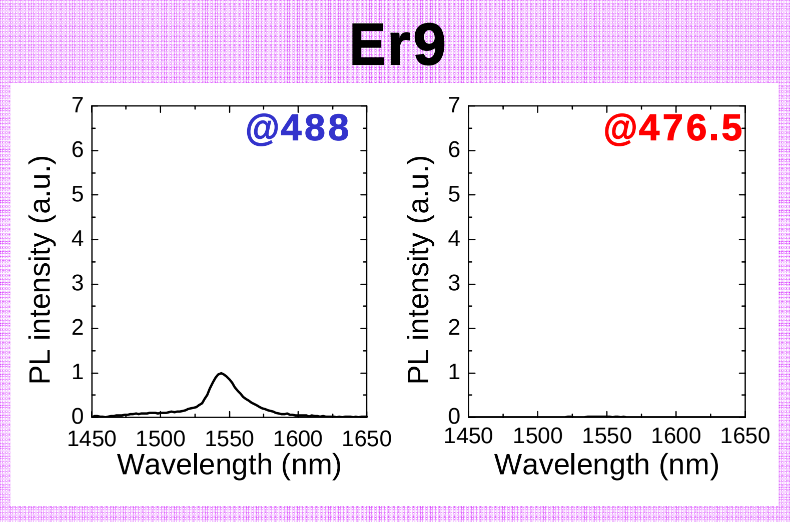


**Ag-exchange process** (1 mol% $AgNO_3$)

✓ Defect production

✓ Ag-O formation

☹ PL intensity decrease

😐 No energy transfer

☹ Lifetime decrease

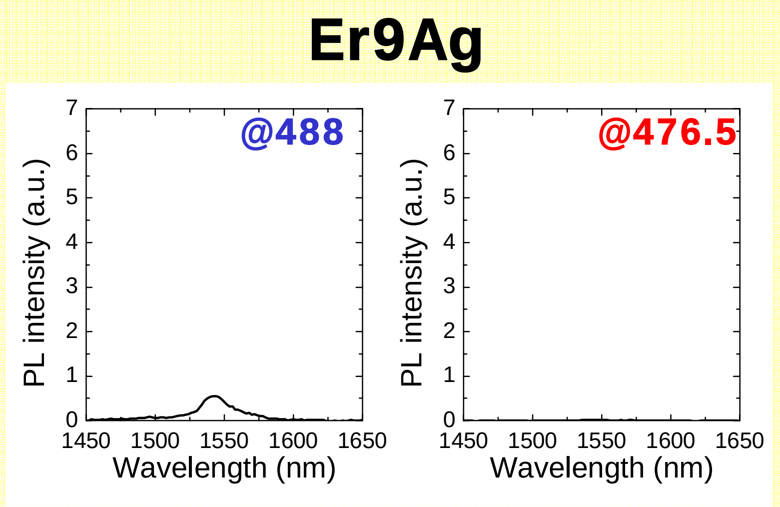

# Er PL emission at 1.54 μm: thermal treatment

| Sample label | PL int. @488 | PL int. @476.5 | Lifetime (ms) |
|---|---|---|---|
| Er9 | 1.0 | ~0 | 11.0 |
| Er9Ag | 0.5 | ~0 | 7.7 |
| Er9Ag-3h500 | 3.0 | 2.9 | 8.0 |
| Er9Ag-5h500 | 3.2 | 3.4 | 8.2 |
| Er9Ag-3h500 1He | 6.1 | 6.5 | 7.2 |
| Er9Ag-3h500 6He | 0.9 | 0.9 | 5.4 |

***PL int.*** *referred to the normalized* ***Er9*** *resonant emision*

## Er9

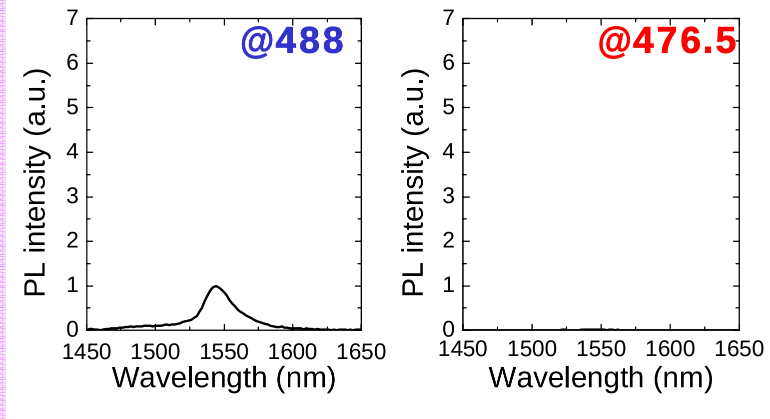


## Annealing treatment (3-5h at 500°C)

- ✓ Matrix recovery
- ✓ Ag aggregates precipitation

⇒

- ☺ PL intensity increase
- ☺ Energy transfer
- ☺ Lifetime increase

## Er9Ag-3h500

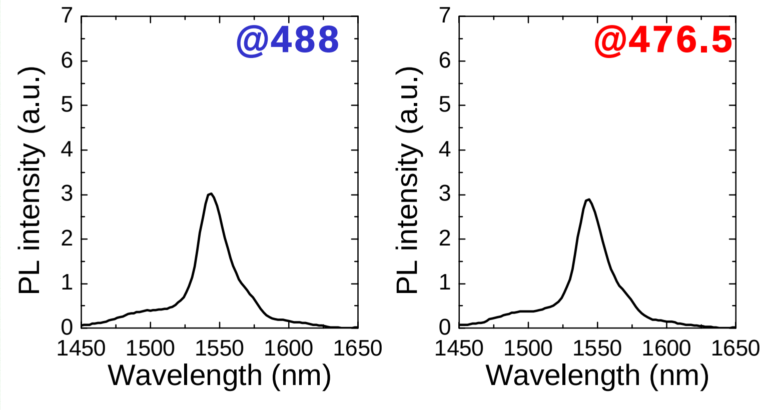

# Local environment around Ag

## **EXAFS** at the Ag K-edge

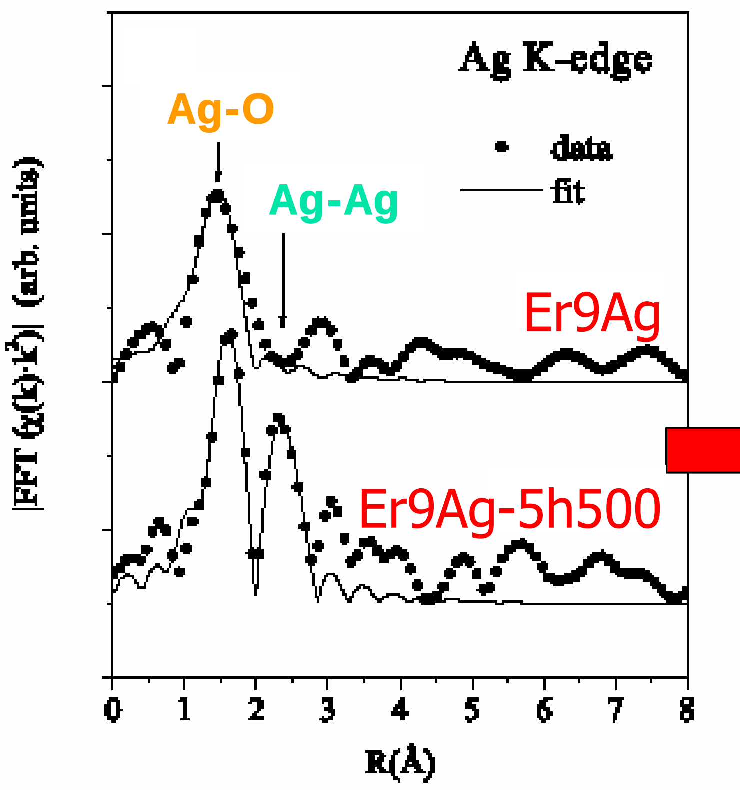


*Moduli of EXAFS Fourier transform spectra*

- ✓ After Ag-exchange only Ag-O coordination detected

| Sample label | Coord. | R (Å) | N | $\sigma^2$ ($\times 10^{-4}$ Å$^2$) |
|---|---|---|---|---|
| Er9Ag | Ag-O | 2.09±0.02 | 1.3±0.3 | 78±41 |
| Er9Ag-5h500 | Ag-O | 2.14±0.05 | 1.4±0.7 | 125±94 |
| | Ag-Ag | 2.72±0.09 | 2±1 | 255±150 |
| Ag foil | Ag-Ag | 2.88±0.02 | 12 | 32±10 |
| $Ag_2O$ powder | Ag-O | 2.05±0.02 | 2 | 22±20 |
| | Ag-Ag | 3.36±0.02 | 12 | 232±34 |

- ✓ Annealing induces the precipitation of Ag aggregates

# Er PL emission at 1.54 μm: low dose $He^+$ irradiation

| Sample label | PL int. @488 | PL int. @476.5 | Lifetime (ms) |
|---|---|---|---|
| Er9 | 1.0 | ~0 | 11.0 |
| Er9Ag | 0.5 | ~0 | 7.7 |
| Er9Ag-3h500 | 3.0 | 2.9 | 8.0 |
| Er9Ag-5h500 | 3.2 | 3.4 | 8.2 |
| Er9Ag-3h500 1He | 6.1 | 6.5 | 7.2 |
| Er9Ag-3h500 6He | 0.9 | 0.9 | 5.4 |

***PL int.*** *referred to the normalized* ***Er9*** *resonant emision*

## Er9Ag-3h500

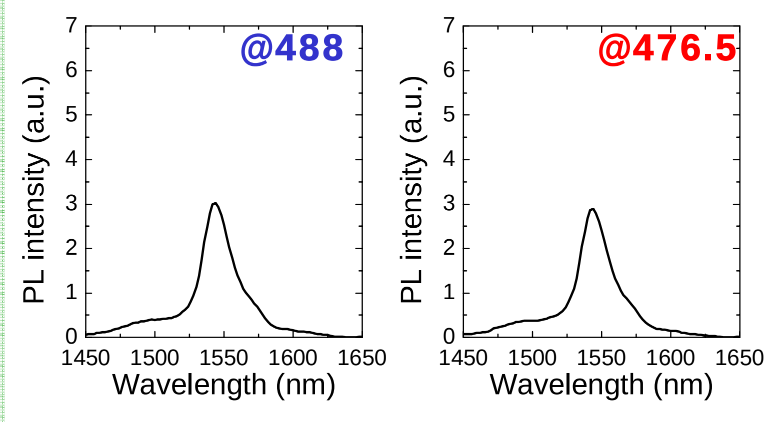


## Low dose irradiation (1×$10^{17}$ $He^+/cm^2$)

- ✓ Defect production
- ✓ More Ag aggregates

☺ PL intensity increase

☺ Energy transfer

☹ Lifetime decrease

## Er9Ag-3h500 1He

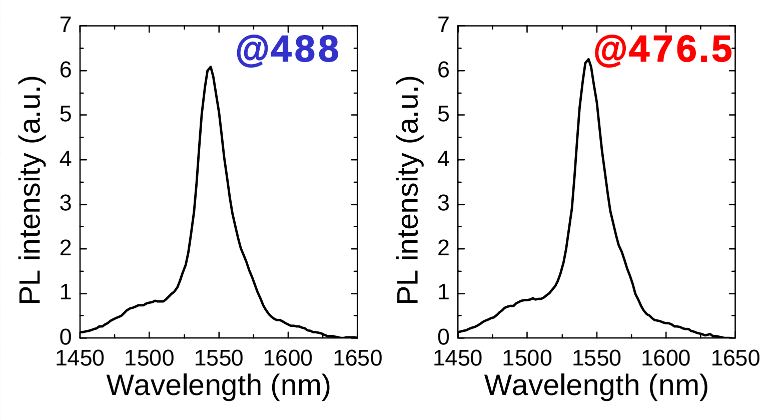

# Er PL emission at 1.54 μm: high dose $He^+$ irradiation

| Sample label | PL int. @488 | PL int. @476.5 | Lifetime (ms) |
|---|---|---|---|
| Er9 | 1.0 | ~0 | 11.0 |
| Er9Ag | 0.5 | ~0 | 7.7 |
| Er9Ag-3h500 | 3.0 | 2.9 | 8.0 |
| Er9Ag-5h500 | 3.2 | 3.4 | 8.2 |
| Er9Ag-3h500 1He | 6.1 | 6.5 | 7.2 |
| Er9Ag-3h500 6He | 0.9 | 0.9 | 5.4 |

***PL int.*** *referred to the normalized* ***Er9*** *resonant emision*

## Er9Ag-3h500

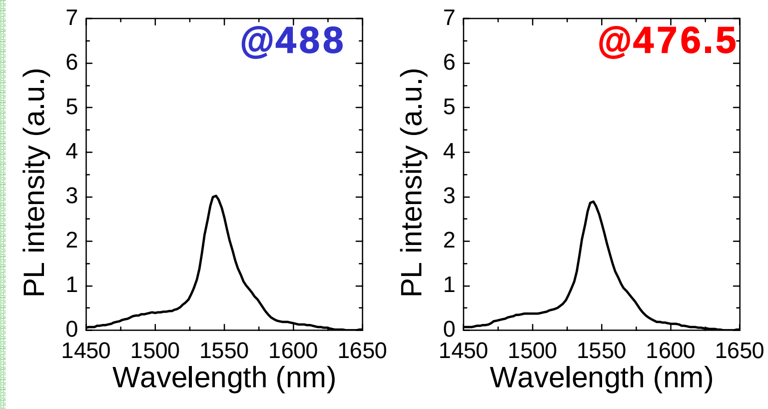


## High dose irradiation ($6\times10^{17}$ $He^+/cm^2$)

- ✓ Massive defect production
- ✓ Formation of large Ag nanoparticles (<D>= 5 nm)

☹ PL decrease

☺ Energy transfer

☹ Lifetime decrease

## Er9Ag-3h500 6He

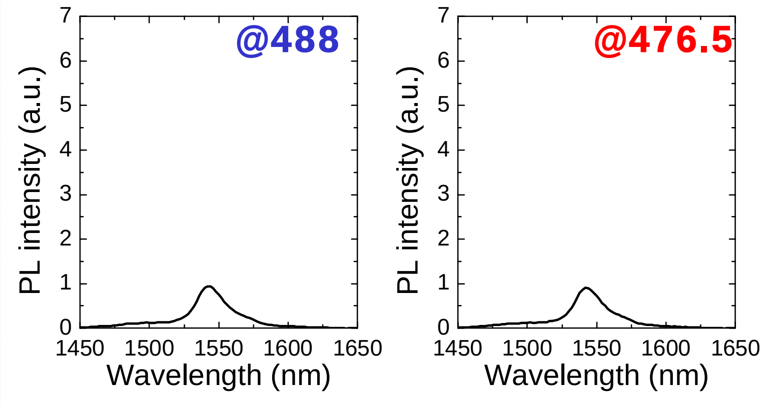

# $He^+$ irradiation: structural investigation

**XRD** in grazing incidence mode

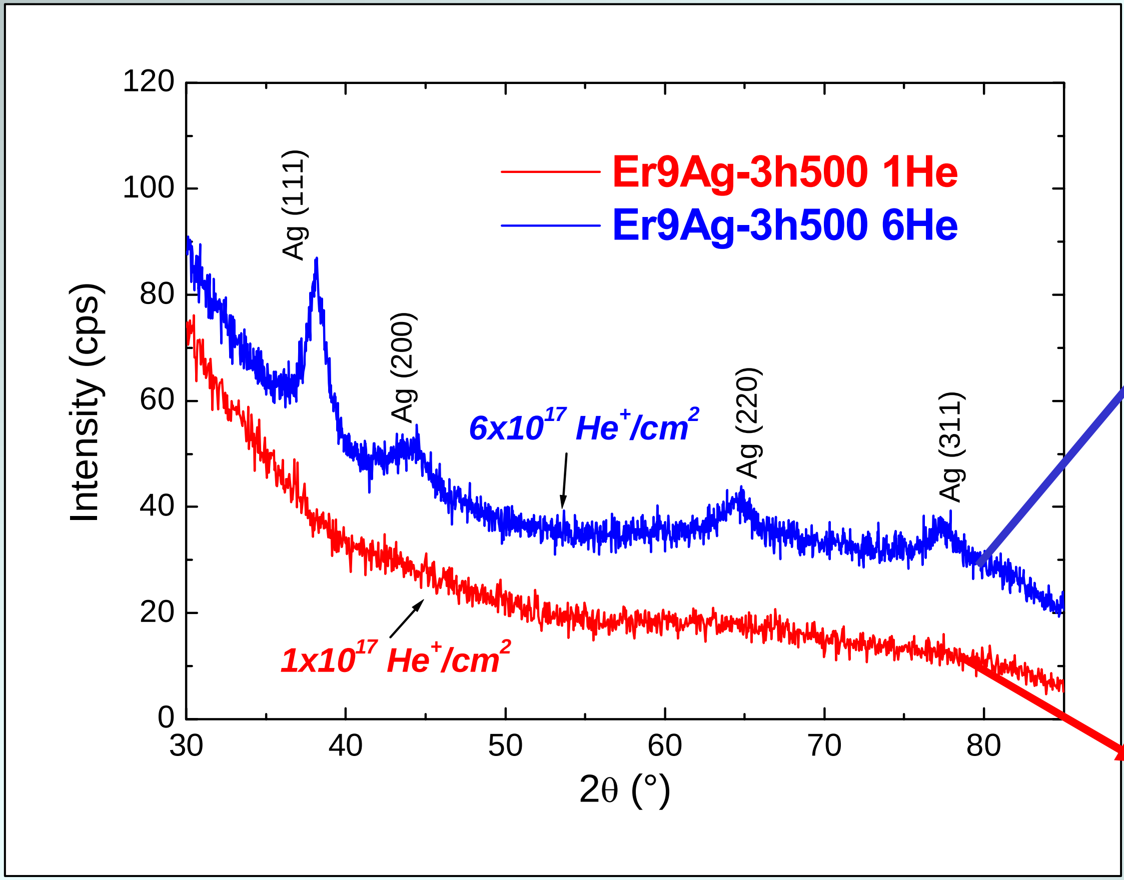


Annealing and
high dose irradiation

Ag nanoparticles
(<D>= 5 nm)

Annealing and
low dose irradiation

**NO** Ag nanoparticle
formation

# PLE measurements

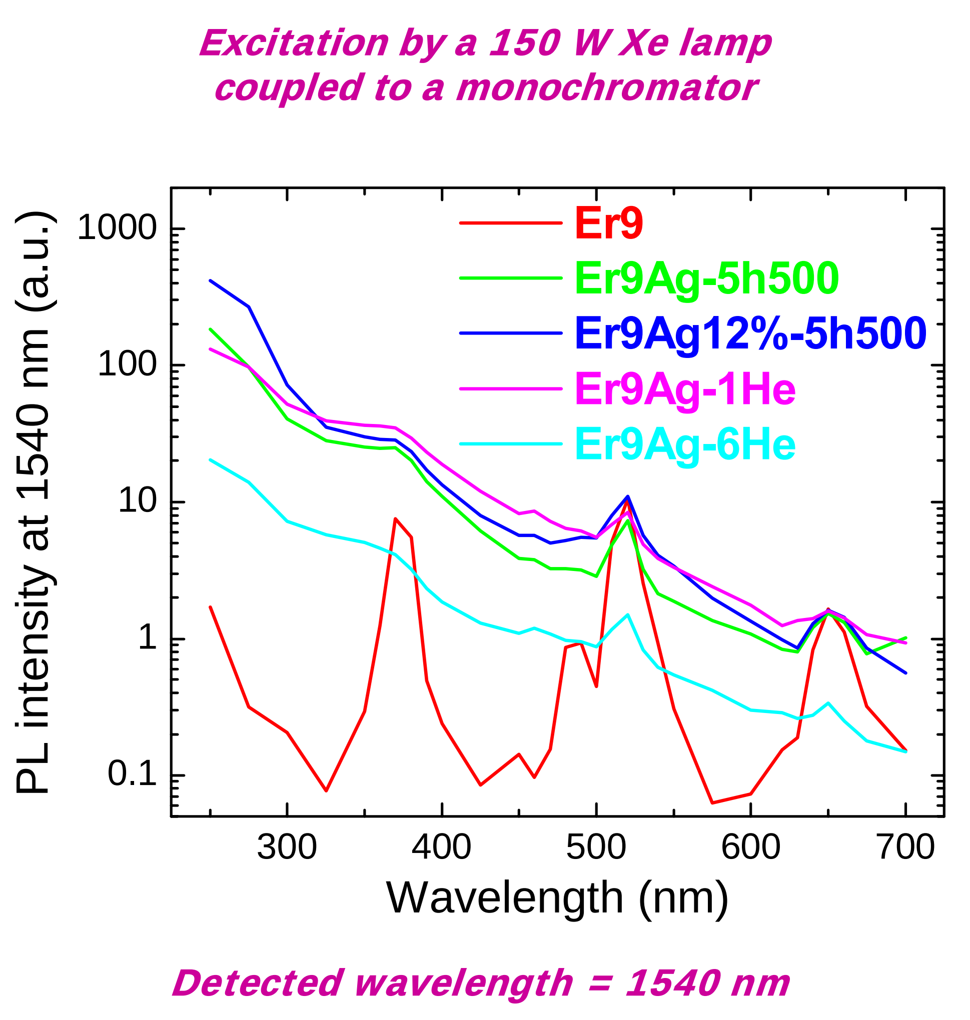


- ✓ Sol-gel sample: $Er^{3+}$ excitation only by direct light absorption
- ✓ Ag-exchanged samples: possibility of broadband $Er^{3+}$ excitation
- ✓ No evidence of Ag SPR features

# Effective cross section evaluation

***Inverse of the risetime as a function of the photon flux***

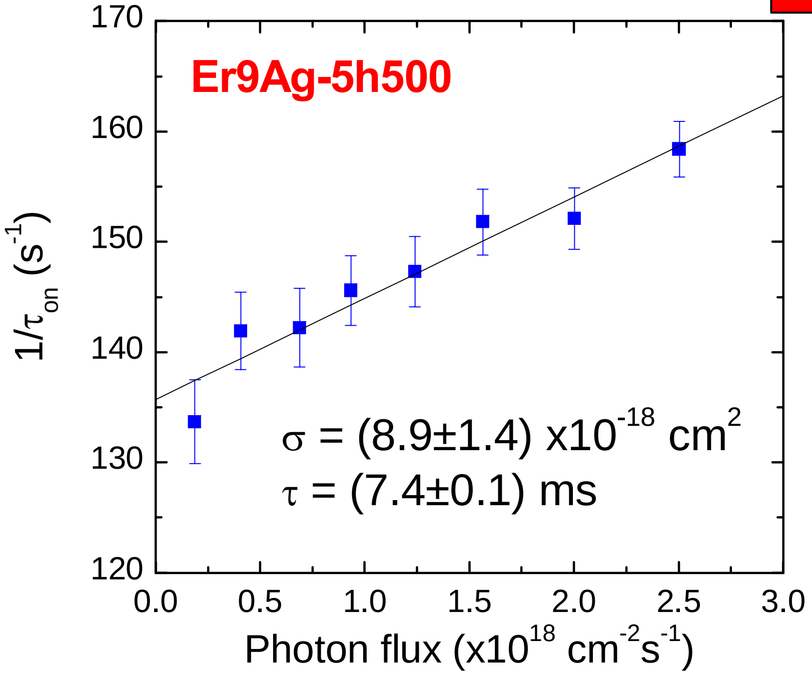


***476.5 nm non-resonant excitation***

Evaluation of the
Ag-mediated effective cross section

***Effective cross section evaluation:***

$$\frac{1}{\tau_{ON}} = \sigma_{eff}\varphi + \frac{1}{\tau}$$

| Sample labels | Cross section ($cm^2$) |
|---|---|
| Er9Ag-5h500 | $(8.9\pm1.4)\times10^{-18}$ |
| Er9Ag(12%)-5h500 | $(8.2\pm1.6)\times10^{-18}$ |

The measured cross section value (~ 8-9×$10^{-18}$ $cm^2$) is many orders of magnitude higher than the one for direct absorption of Er ions in silica (~ $10^{-20}$-$10^{-21}$ $cm^2$)

# Waveguiding properties

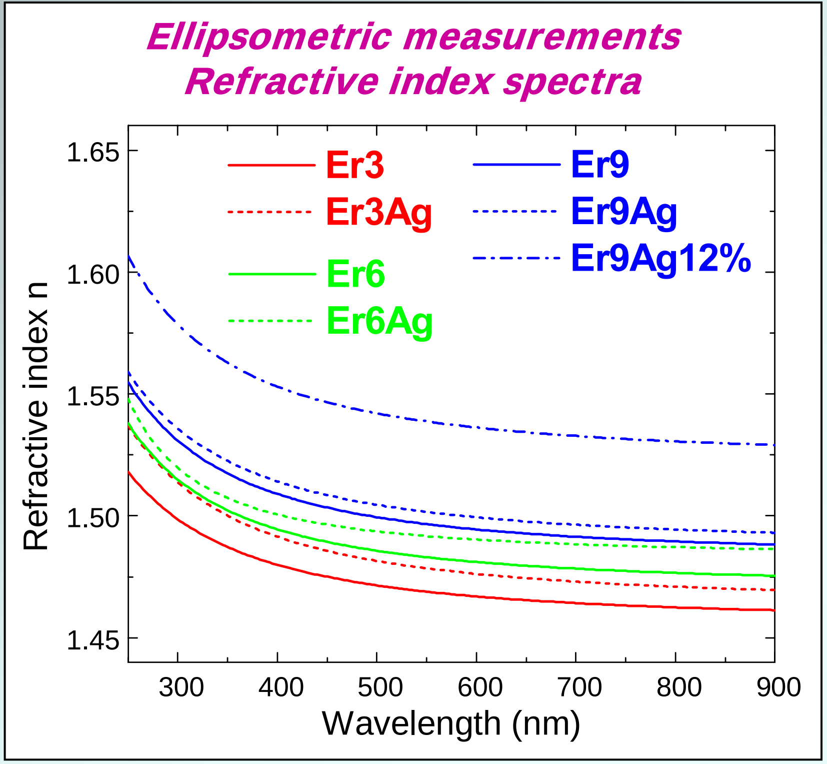


✓ Larger refractive index as the Na concentration increases (*Er3* → *Er9*)

✓ Larger refractive index after Ag ion incorporation

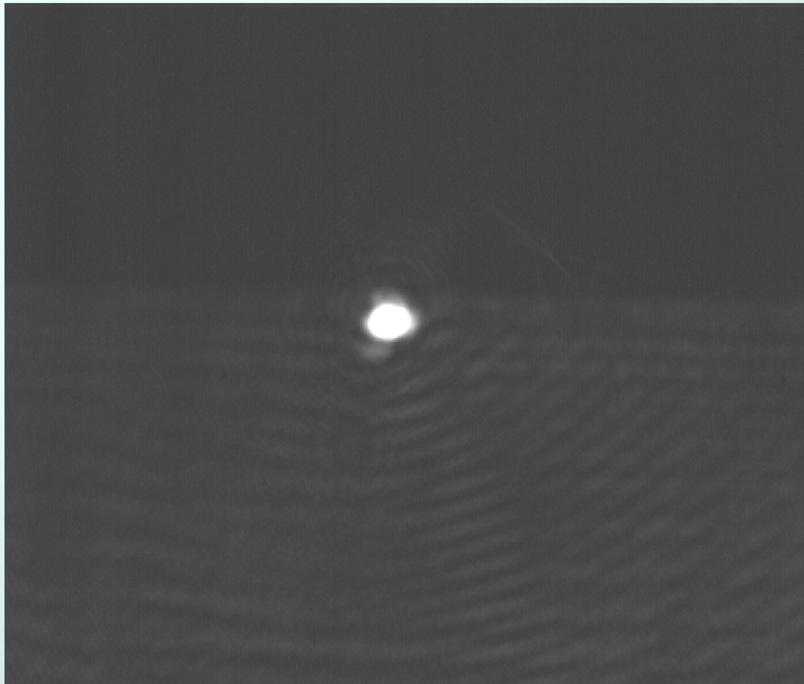

Near field image of a propagation mode at 1.02 μm in a 1.5 μm height × 9 μm width ion-exchanged channel waveguide

Conclusions

# Conclusions

- ✓ Enhancement of emission at 1.54 μm in Er and Ag/Au codoped system
- ✓ Small metal aggregates act as effective Er sensitizers
- ✓ $Er^{3+}$ sensitization through an energy transfer process
- ✓ Possibility of $Er^{3+}$ excitation in a wide range of wavelength
- ✓ Increase of the effective cross section (up to ~$10^{-17}$-$10^{-18}$ $cm^2$ at 488 nm)

Work in progress:

- ★ Deeper comprehension of the mechanism involved in Er-metal interaction
- ★ Investigation of metal optical activity (Au)
- ★ Possibility to sensitize $Er^{3+}$ through the interaction with other metal species
- ★ Optimization of material synthesis conditions to improve optical behaviour
- ★ Feasibility of a waveguide amplifier device

# General conclusions

- ✓ Enhancement of emission at 1.54 μm in Er and Ag/Au codoped system
- ✓ Small metal aggregates act as effective $Er^{3+}$ sensitizers
- ✓ $Er^{3+}$ sensitization through of an energy transfer process
- ✓ Possibility of $Er^{3+}$ excitation in a wide range of wavelength
- ✓ Effective cross section of ~$10^{-17}$-$10^{-18}$ $cm^2$ (Er in silica ~ $10^{-20}$-$10^{-21}$ $cm^2$)

*Technological remark*

Cheap flashlamps could be used instead of the expensive 980 nm or 1540 nm lasers common in today's commercial Er doped devices

Work in progress:

- ★ Deeper comprehension of the mechanism involved in Er-metal interaction
- ★ Investigation of metal optical activity (Au)
- ★ Possibility to sensitize Er through the interaction with other metal species
- ★ Optimization of material synthesis conditions to improve optical behaviour
- ★ Feasibility of a waveguide amplifier device